### *PA-7.1.3 Brine Flow Out of the Repository*

***The anhydrite MBs and the shafts provide possible pathways for brine flow away from the repository in the undisturbed scenario (S1). The Salado flow model only tabulates the volume of brine crossing boundaries within the model grid; it does not identify whether the brine contains radionuclides from the waste. Transport is calculated separately from the flow and is discussed in Section PA-7.2.***

***Figure PA-43 shows cumulative brine outflow from the excavated regions of the repository (BRNREPOC). Brine flow out of the DRZ into the MBs is shown in Figure PA-44, and flow up the shaft to the bottom of the Culebra is shown in Figure PA-45. Comparison of total cumulative brine outflow into all MBs (BRAALOC, Figure PA-44) to total outflow (Figure PA-43) confirms that the primary path for brine outflow is along the MBs.***

***The distribution of brine flow among the potential pathways varies somewhat between vectors, but typically outflow along MB 139 to the south accounts for most of the total brine outflow. The dominance of MB 139 to the south as the primary conduit for brine outflow is illustrated in Table PA-26, which tabulates maximum brine outflow along each potential pathway for any vector in replicate R1. MB 139 is down the stratigraphic dip, and, being the lowest outflow pathway, it is most frequently saturated.***

***Figure PA-46 shows the volumes of brine that cross the LWB through the MBs. The largest outflow across the LWB is 433 $m^3$. Table PA-26 shows that a smaller volume of brine (50 $m^3$) may reach the Culebra through the shaft. Brine crossing the LWB or moving up the shaft does not necessarily indicate releases from the repository, since the brine may not have been in contact with the waste; the brine may have been present in the MBs at the start of the regulatory period. Section PA-7.2 presents the results of the transport calculations that determine the amount of radionuclides that be released by transport in brine.***

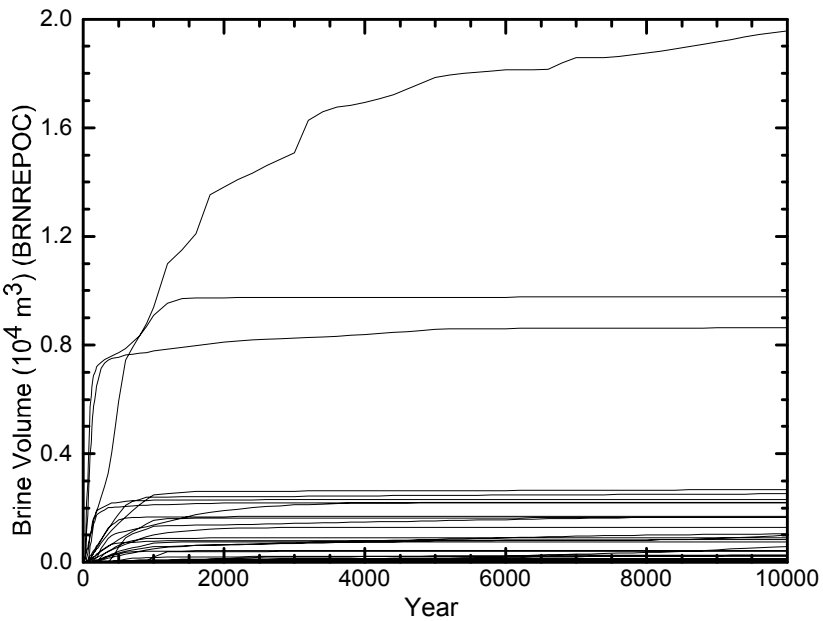


***Figure PA-43. Brine Flow Away from the Repository, Replicate R1, Scenario S1.***

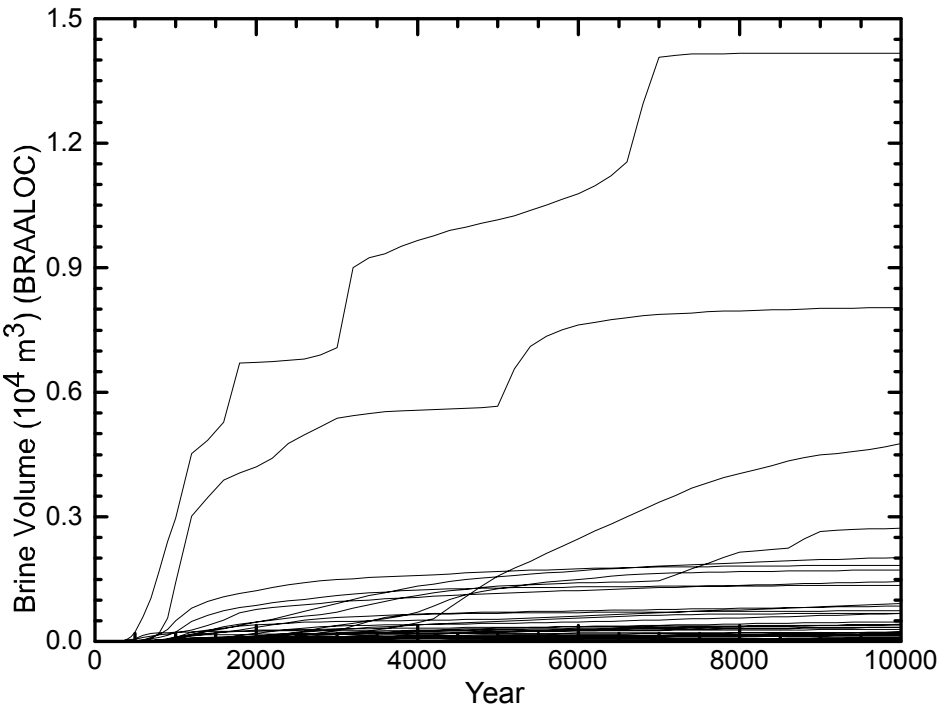


***Figure PA-44. Brine Flow Away from the Repository Via All Marker Beds, Replicate R1, Scenario S1.***

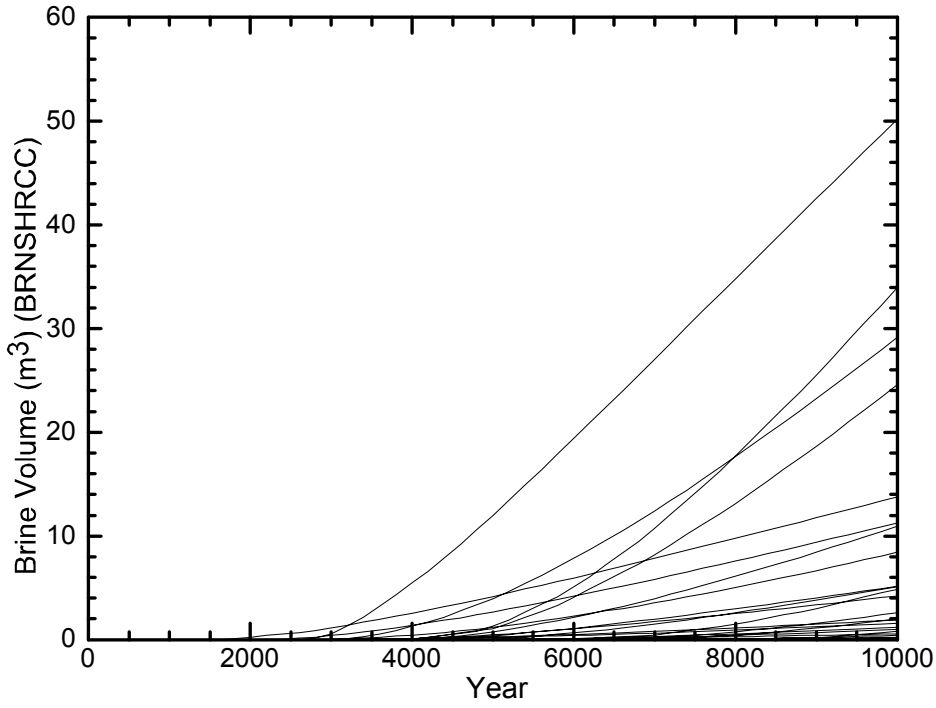


***Figure PA-45. Brine Outflow Up the Shaft, Replicate R1, Scenario S1.***

***Table PA-26. Volume of Brine Outflow by Various Potential Pathways***

| *Pathway for Brine Outflow* | *Maximum ($m^3$)* |
|---|---|
| *MB 138 North* | *432* |
| *MB 138 South* | *1,567* |
| *Anhydrite AB North* | *0* |
| *Anhydrite AB South* | *5* |
| *MB 139 North* | *1,832* |
| *MB 139 South* | *12,828* |
| *Shaft (to base of Culebra)* | *50* |

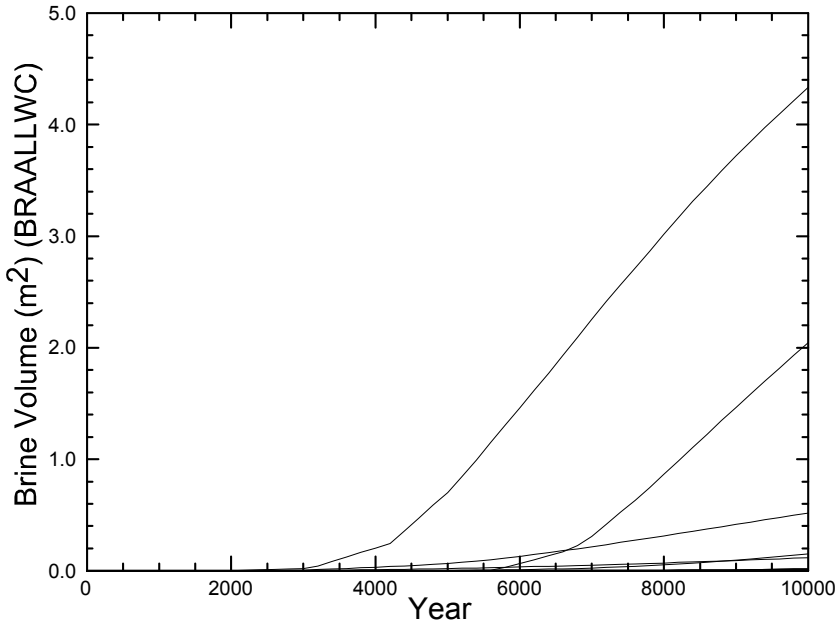


***Figure PA-46. Brine Flow Via All MBs Across The LWBs, Replicate R1, Scenario S1.***

***Regression between total cumulative brine flow into the MBs (BRAALOC) and the uncertain parameters in the LHS (Figure PA-47) shows that uncertainty in brine outflow into the MBs is primarily determined by WMICDFLG, which indicates whether microbial gas generation is modeled and what materials, if any, are consumed. The positive correlation of WMICDFLG with BRAALOC is comparable to the correlation of WMICDFLG with pressure in the waste panel (WAS_PRES) indicating that increasing pressure correlates with increasing brine flow into the marker beds. The PRCC for WMICDFLG is approximately 0.85 throughout the 10,000-year calculation time, indicating that uncertainty in this parameter explains roughly 85% of the variability in BRAALOC. The porosity of halite (HALPOR) accounts for most of the remaining uncertainty. Increasing HALPOR means that more brine is available in the DRZ for inflow into the repository, and brine inflow is a necessary precursor to outflow. The influence of the other three parameters listed in Figure PA-47 is negligible.***

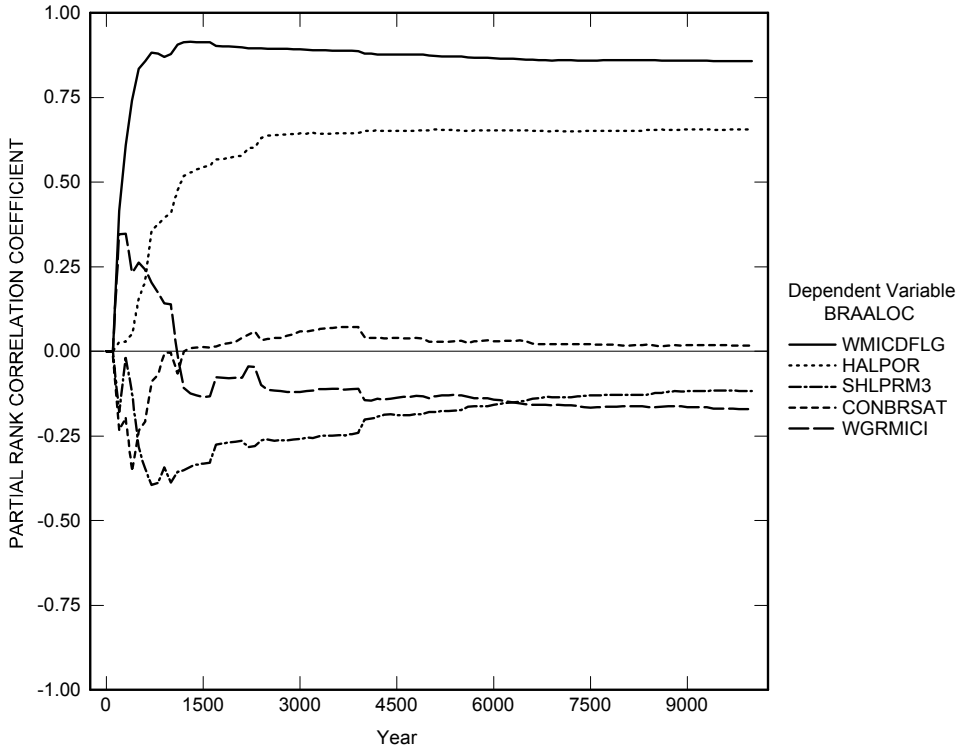


***Figure PA-47. Primary Correlations of Total Cumulative Brine Flow Away from the Repository Through All MBs with Uncertain Parameters, Replicate R1, Scenario S1.***

***Figure PA-48 compares statistics of brine outflow from the repository for the three replicates, and shows that all three replicates produce similar results. The BRNREPOC provides a more valid basis for comparison among the replicates than the other outflow variables, because it has fewer vectors with zero values.***

## *PA-7.2 Radionuclide Transport*

***Radionuclide transport in the undisturbed scenario is calculated by the code NUTS. Screening runs are used to determine which vectors have the potential to transport radionuclides to the accessible environment (see Section PA-6.7.2). Full transport simulations are run for all vectors that are screened in. This section summarizes the transport results for the undisturbed repository, both up the shaft to the Culebra, and through the Salado to the LWB. Lowry (2003) presents a detailed analysis of NUTS results for the CRA-2004 PA.***

### *PA-7.2.1 Transport to the Culebra*

***No vectors showed any amount of radionuclide transported to the Culebra through the shafts from the undisturbed repository. Consequently, no radionuclides can transport through the Culebra to the LWB in undisturbed conditions.***

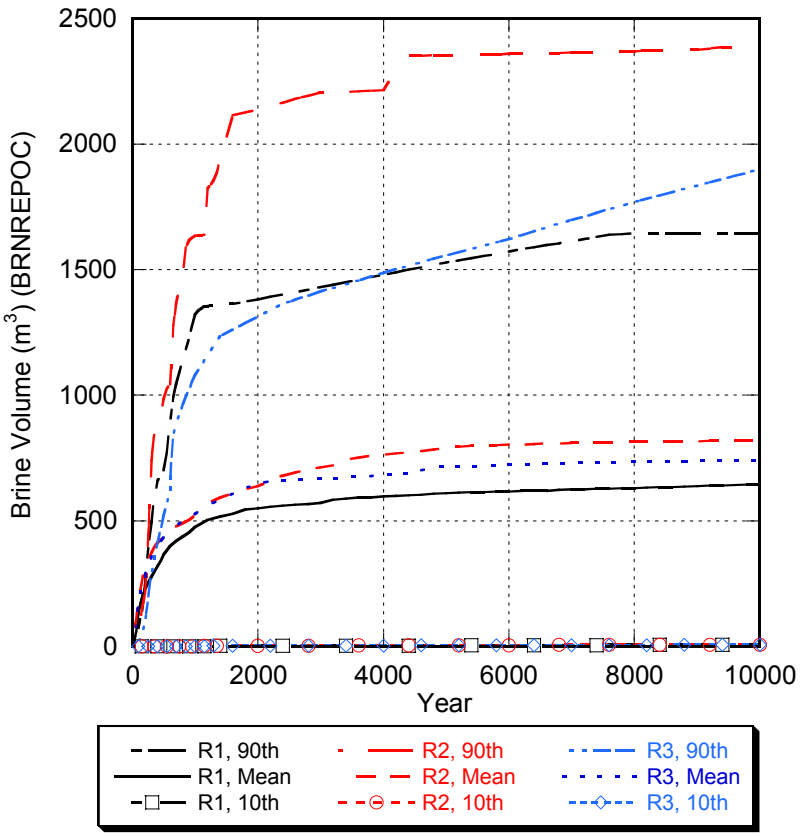


***Figure PA-48. Comparison of Brine Flow Away from the Repository between Replicates, Scenario S1.***

### *PA-7.2.2 Transport to the Land Withdrawal Boundary*

***In all three replicates (300 vectors) of the CRA-2004 PA, only one vector displayed non-zero releases across the LWB from the undisturbed repository. Vector 82 of Replicate R1 released a total of $2.89 \times 10^{-15}$ EPA units out the southern anhydrite MB 139 over 10,000 years. The release is predominately $^{239}$Pu. In this vector, quantities of all of the isotopes move through the MB about 677 m. However, at 984 m from the edge of the repository the concentration of $^{239}$Pu decreases to less than $1 \times 10^{-7}$ EPA units. The total distance from the repository edge to the LWB is 2,400 m. Thus, the non-zero release in this vector is indicative of numerical dispersion resulting from the coarse grid spacing between the repository and the LWB, rather than a probable transport of radionuclides.***

***The releases from the undisturbed scenario are insignificant when compared to releases from drilling intrusions (see Section PA-9.0). Consequently, releases in the undisturbed scenario are omitted from the calculation of total releases from the repository (see Section PA-9.0) to satisfy the containment requirements of 40 CPR Part 194. Chapter 8.0 demonstrates that WIPP complies with the individual protection requirements of 40 CFR § 191.15 and the groundwater protection requirements of 40 CFR Part 191, Subpart C.***

# *PA-8.0 RESULTS FOR A DISTURBED REPOSITORY*

***The WIPP repository might be disturbed by exploratory drilling for natural resources during the 10,000-year regulatory period. Drilling could create additional pathways for radionuclide transport, especially in the Culebra, and could release material directly to the surface. In addition, mining for potash within the LWB might alter flow in the overlying geologic units and may accelerate transport through the Culebra. The disturbed scenarios used in PA modeling capture the range of possible releases resulting from drilling and mining.***

***As outlined in Section PA-6.8, total releases are computed by the code CCDFGF, which evaluates the function f in Equation (24) for each stochastically generated future of the repository. Total releases comprise transport releases and direct releases. Transport releases generally involve movement of radionuclides up an abandoned borehole into the Culebra, then through the Culebra to the LWB. Transport of radionuclides to the Culebra is computed using the codes NUTS and PANEL (see Section PA-4.3 and Section PA-4.4, respectively) using the brine flows computed by BRAGFLO. Transport through the Culebra is computed by the code SECOTP2D (see Section PA-4.9) using flow fields calculated by MODFLOW (see Section PA-4.8).***

***Direct releases occur at the time of a drilling intrusion and include releases of solids (cuttings, cavings, and spallings) computed using the code CUTTINGS_S (see Section PA-4.5 and Section PA-4.6) and direct releases of brine computed using BRAGFLO (see Section PA-4.7). Pressure and brine saturation within the waste are initial conditions to the models for direct releases. Results from the undisturbed repository (see Section PA-7.0) are used as the initial conditions for the first intrusion. To calculate initial conditions for subsequent intrusions, and to compute the source of radionuclides for transport in the Culebra, a set of drilling scenarios are used to calculate conditions within the repository after an intrusion, using BRAGFLO (Section PA-6.7.1).***

***This section first summarizes the scenarios used to represent drilling intrusions and the resulting repository conditions calculated by BRAGFLO. Next, transport releases are presented, followed by cuttings and cavings, spallings, and DBRs. Finally, total releases from the repository are summarized.***

## *PA-8.1 Drilling Scenarios*

***As described in Section PA-3.9, the PA considers two types of drilling intrusions, E1 and E2. The E1 scenario represents the possibility that a borehole connects the repository with a pressurized brine reservoir located within the underlying Castile formation. The E2 scenario represents a borehole that does not connect the repository with an underlying brine reservoir. Repository conditions are calculated for the E1 scenario at 350 and 1,000 years, referred to as the BRAGFLO S2 and S3 scenarios, respectively. The BRAGFLO scenarios S4 and S5 represent E2 drilling events that occur at 350 and 1,000 years, respectively. An additional BRAGFLO scenario, S6, simulates the effects of an E2 intrusion at 800 years followed by an E1 intrusion 1,200 years later into the same panel. For more details on the BRAGFLO scenarios, see Section PA-6.7.1.***

### *PA-8.2 Mining Scenarios*

***Long-term releases within the Culebra could be influenced by future mining activities that remove all the known potash reserves within the LWB and cause the transmissivity within the overlying Culebra to change. As outlined in Section PA-3.8, full mining of known potash reserves within the LWB in the absence of active and passive controls occurs with a probability specified as a Poisson process with a rate of $10^{-4}$ $yr^{-1}$. For any particular future $x_{st}$ in $S_{st}$, this rate is used to define a time $t_{min}$ at which full mining has occurred. As described in Section PA-6.8.7, flow fields are calculated for the Culebra for two conditions: partial mining, which assumes that all potash as been mined from reserves outside the LWB; and full mining, which assumes all reserves have been mined both inside and outside the LWB. Transport through the Culebra uses the partial mining flow fields prior to $t_{min}$, and the full mining flow fields after $t_{min}$.***

### *PA-8.3 Salado Flow*

***This section summarizes the results of the Salado flow calculations for the disturbed scenarios. Stein and Zelinski (2003b) provide a detailed presentation on the BRAGFLO model, calculation results, and further sensitivity analyses***

#### *PA-8.3.1 Pressure in the Repository*

***Figure PA-49 shows pressure in the waste panel (WAS_PRES for area Waste Panel of Figure PA-8) for the 100 vectors of replicate R1 for each BRAGFLO scenario (Table PA-21). Scenario S1 represents undisturbed repository conditions; the pressure in the waste panel in scenario S1 (Figure PA-49a) is analyzed in Section PA-7.1. Before the drilling intrusions at 350 or 1,000 years, repository pressure increases as described in Section PA-7.1.***

***After the intrusion, pressure exhibits patterns that vary depending on the type of intrusion and upon sampled input variables related to the intrusion.***

***Scenarios S2 and S3 represent E1 intrusions at 350 and 1,000 years, respectively (Table PA-21). At the time of the intrusion, brine flow from the Castile brine reservoir leads to an increase in pressure (Figure PA-49b and c). However, pressure drops sharply 200 years after the intrusion when the borehole plugs above the repository fail (Table PA-5) and the permeability of the borehole generally increases. However, in vectors with low borehole permeability after plug failure, pressure does not change noticeably as a result of the borehole plug failure. Twelve hundred years after the drilling intrusion, the permeability of the borehole connecting the repository to the Castile is reduced by an order of magnitude because of creep closure (Table PA-5). This material change reduces pressure slightly in some vectors, but does not appear to have a significant effect on the pressure in most vectors.***

***Scenarios S4 and S5 represent E2 intrusions at 350 years and 1,000 years, respectively. The borehole plugs effectively prevent any change in repository pressure from the time of the intrusion until the borehole plugs fail (Figure PA-49d and e). As in the scenarios for E1 intrusions, pressure generally drops sharply when the plugs fail, except for vectors with low borehole permeability after plug failure.***

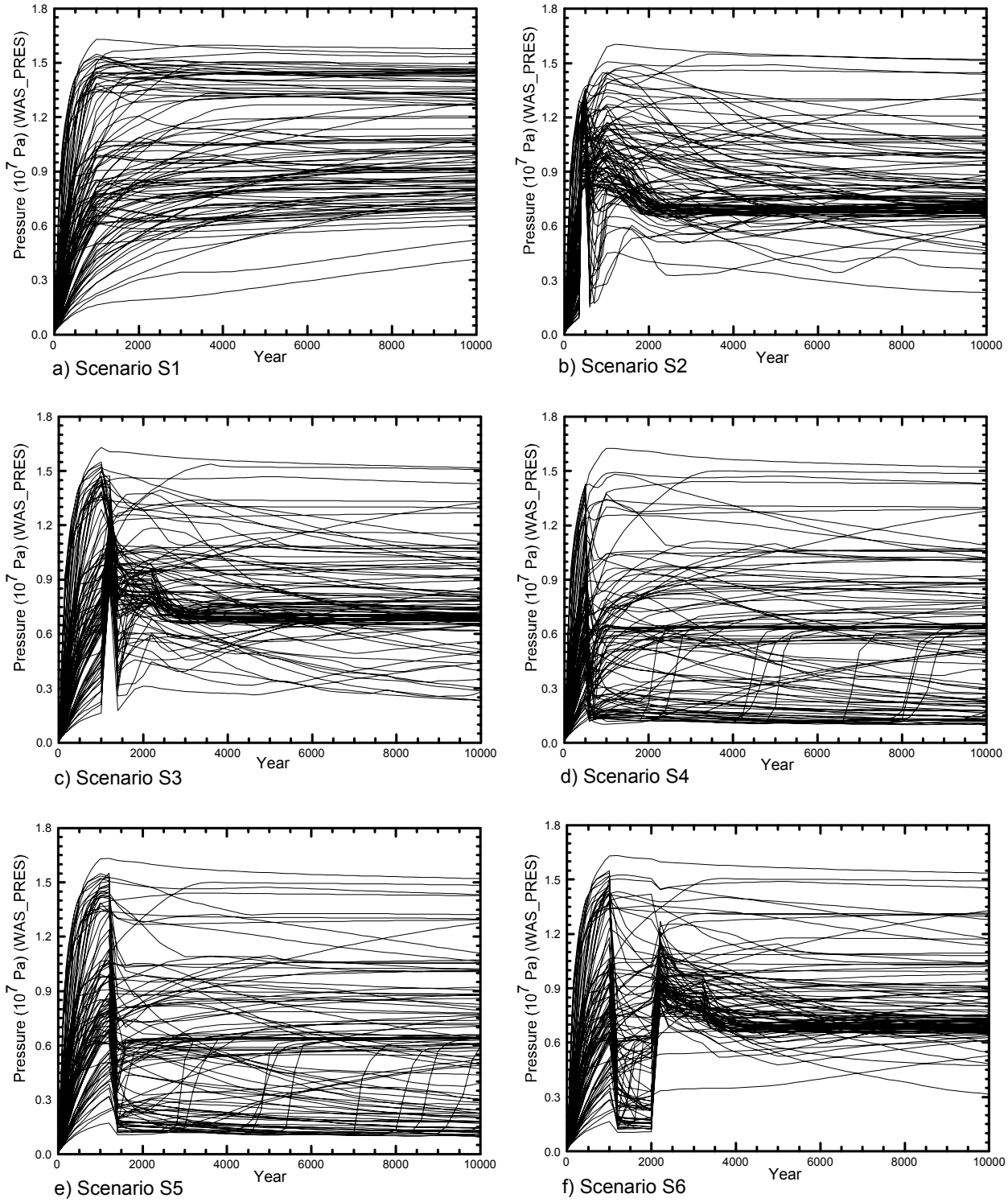


***Figure PA-49. Pressure in the Waste Panel for All Scenarios, Replicate R1.***

***Scenario S6 represents two intrusions into the same panel: an E2 intrusion at 800 years followed by an E1 intrusion at 2000 years. Figure PA-49f shows pressure in the panel for the S6 scenario. The changes in pressure after the first intrusion are nearly identical to that observed in Scenario S5 (Figure PA-49e). In most vectors, the pressure decreases so much that there is a sharp increase in pressure at the time of the second intrusion, which connects the waste panel to the Castile brine reservoir. The changes in pressure after the second intrusion are very similar to those predicted after an E1 intrusion (Scenario S3, Figure PA-49c).***

***Figure PA-50 shows pressure in the rest of repository areas (SRR_PRES for area South RoR and NRR_PRES for area North RoR in Figure PA-8) and in the nonwaste areas (NWA_PRES averaged over areas Ops and Exp in Figure PA-8) for Scenarios S2 and S5, which represent E1 and E2 drilling intrusions into the waste panel at 350 and 1,000 years, respectively. In general, pressure in the rest of repository and nonwaste areas is not immediately affected by the intrusion. The presence of the Option D panel closures (see Section PA-4.2.8) inhibits flow of gas and brine between the intruded panel and adjoining areas, moderating the effects of the intrusion.***

***Figure PA-51 compares mean pressure in the waste panel among the scenarios. Pressure in the disturbed scenarios tends to be lower after the intrusion than pressure in the undisturbed scenario due to the borehole connection to the surface. By 2,000 years after the intrusion, the mean pressure after an E1 intrusion (Scenarios S2, S3, and S6) is about 80 percent of the mean pressure in undisturbed conditions (Scenario S1), and the mean pressure after an E2 intrusion (scenarios S4 and S5) is 60 percent of the mean pressure in undisturbed conditions.***

***Figure PA-52 illustrates the differences in pressure among the various excavated regions after an E1 intrusion at 350 years (Scenario S2). Following the intrusion, mean pressure in the waste panel (WAS_PRES) is temporarily higher than in the other repository regions. About 1,500 years after the intrusion, mean pressure in the South RoR (SRR_PRES) and North RoR (NRR_PRES) is approximately equal to mean pressure in the waste panel. Mean pressure in the nonwaste regions (NWA_PRES) is lower than pressure in the waste-filled regions until about 4,000 years after the intrusion. The delay in pressure equalization between different repository regions is due to the panel closures, which tend to prevent rapid exchange of brine and gas between regions (Hansen et al. 2002) unless pressure exceeds the fracture initiation pressure (approximately 12-14 MPa) after which pressure can rapidly equalize among the regions.***

***Regression between pressure in the waste panel for an E1 intrusion at 350 years (Scenario S2) and the uncertain parameters in the analysis (Section PA-5.2) shows that the uncertainty in the permeability of the borehole (BHPERM) is largely responsible for the uncertainty in pressure after the borehole plugs fail (Figure PA-53). Before the borehole plugs fail, pressure is most sensitive to variations in the initial pressure in the Castile (BPINTPRS) and the indicator for microbial gas generation (WMICDFLG). Increases in BPINTRS can increase brine flow from the Castile to the repository; larger values of WMICDFLG indicate the potential to generate additional gas as a consequence of the additional brine flowing into the***

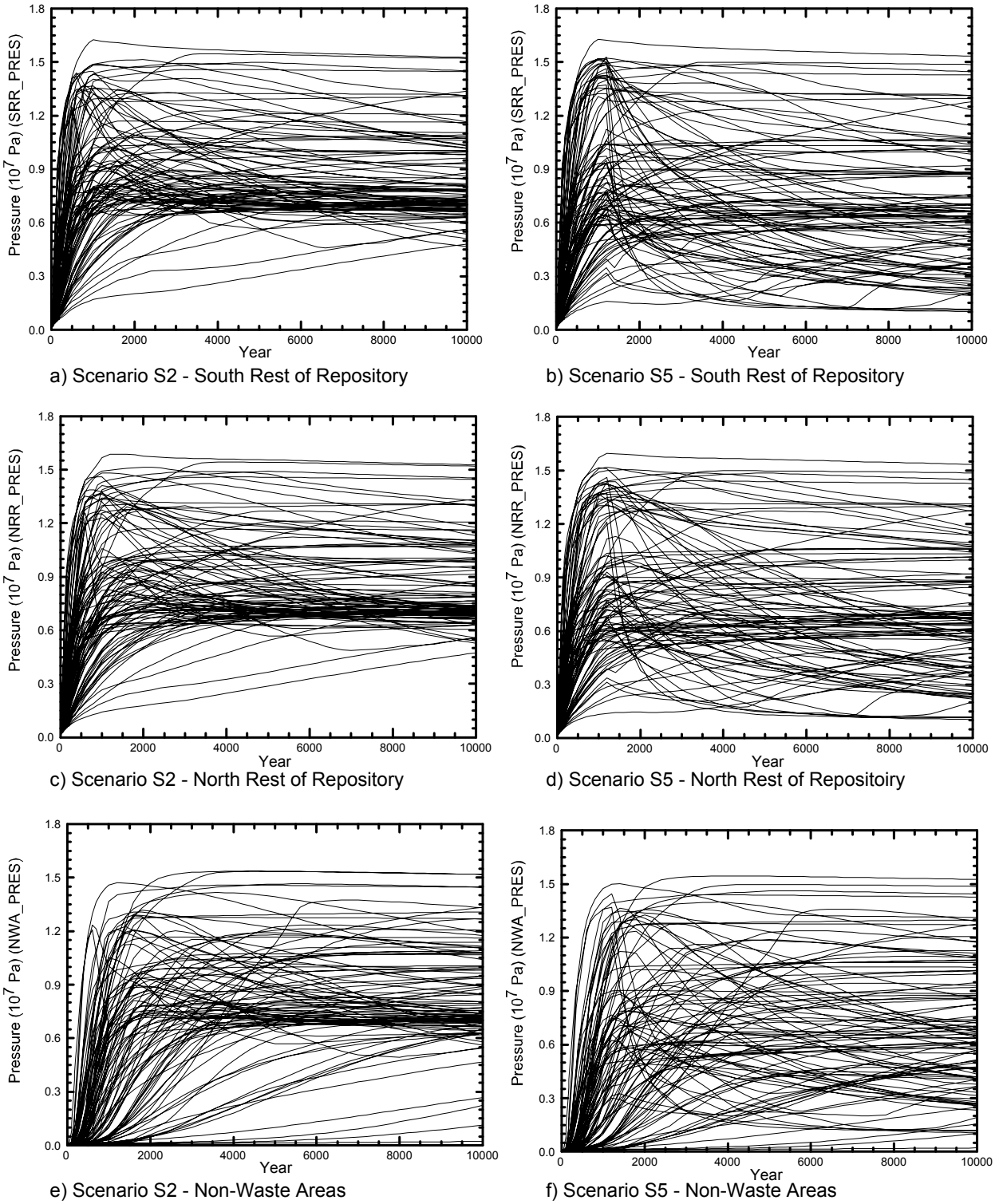


***Figure PA-50. Pressure in Various Regions, Replicate R1, Scenarios S2 And S5.***

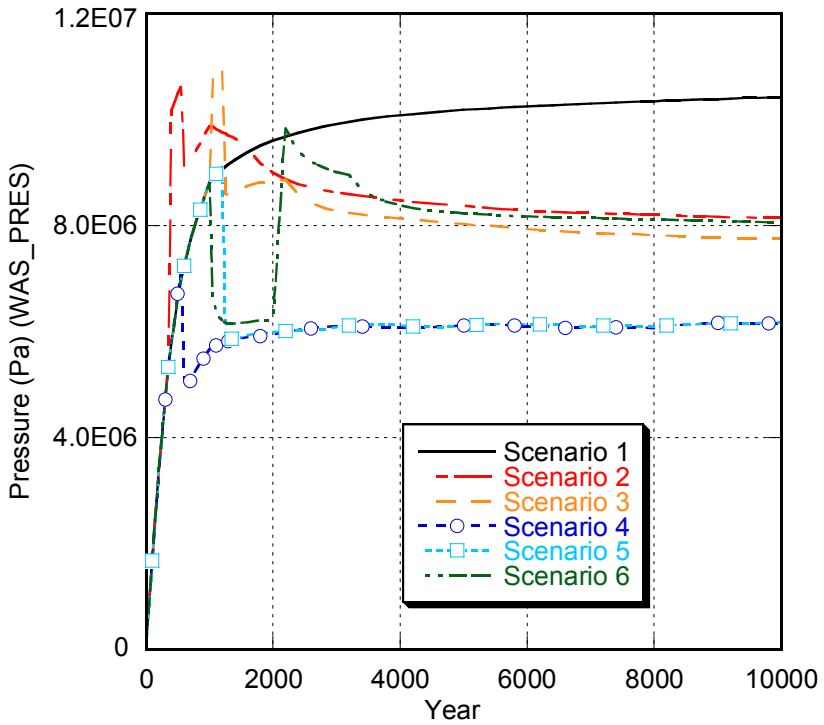


***Figure PA-51. Mean Pressure in the Waste Panel for All Scenarios, Replicate R1***

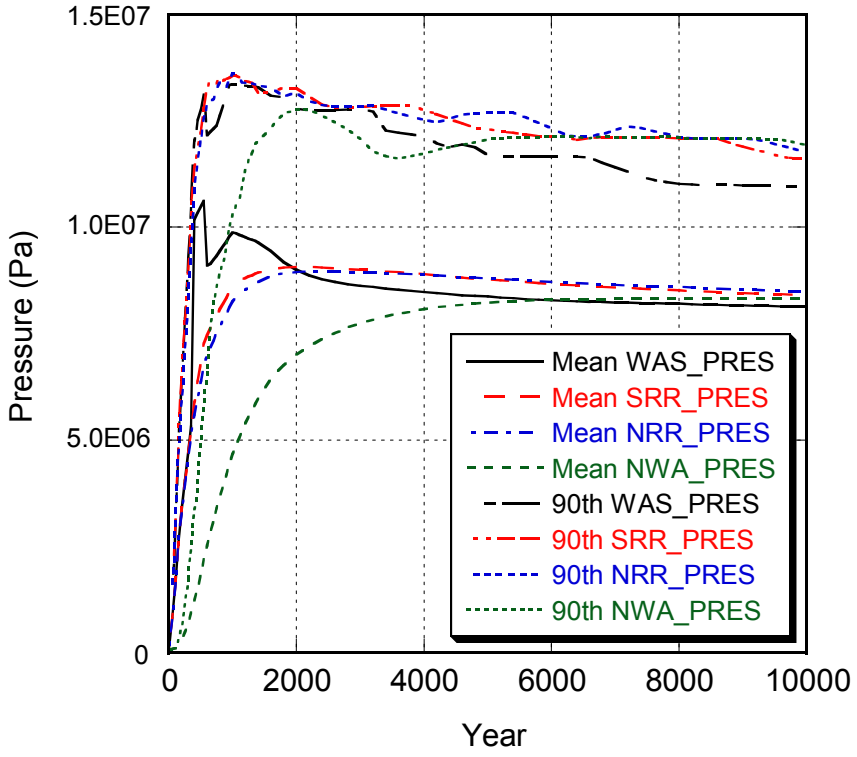


***Figure PA-52. Mean And 90th Percentile Values For Pressure In The Excavated Regions Of The Repository, Replicate R1, Scenario S2.***

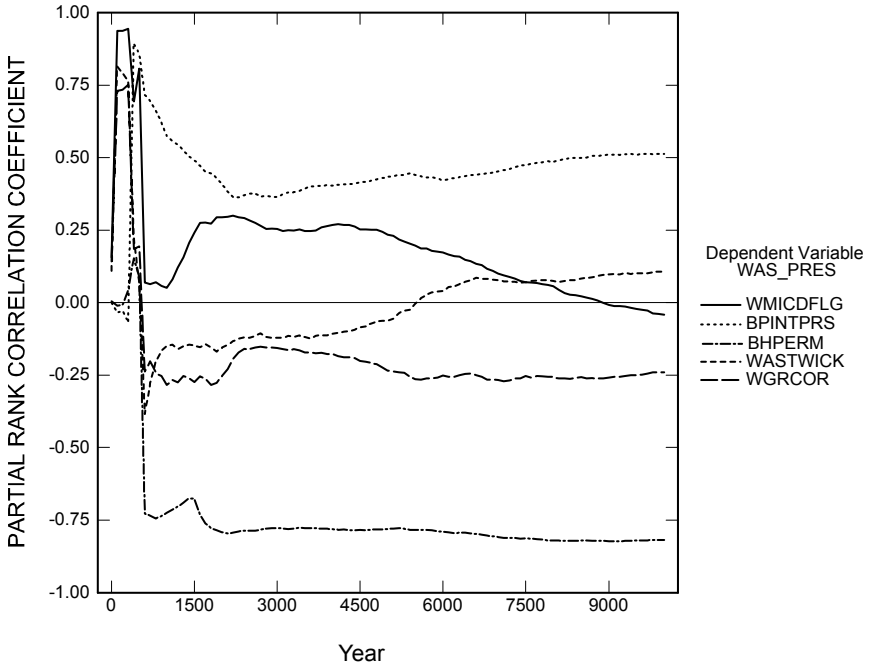


***Figure PA-53. Primary Correlations For Pressure In The Waste Panel With Uncertain Parameters, Replicate R1, Scenario S2.***

***repository. Figure PA-54 shows the regression analysis results for an E2 intrusion at 1,000 years (Scenario S5). As in the analysis of Scenario S2, before the intrusion, the uncertainty in the indicator for microbial gas generation (WMICDFLG) is most important; after the borehole plugs fail, uncertainty in the permeability of borehole fill (BHPERM) is most important. Regression analyses for an E1 intrusion at 1,000 years and for an E2 intrusion at 350 years lead to similar conclusions (Stein and Zelinski, 2003b).***

***Figure PA-55 compares statistics for pressure in the waste panel for scenario S2 among the three replicates, and show that the three replicates produced statistically similar results.***

### *PA-8.3.2 Brine Saturation*

***Brine saturation tends to increase after a drilling intrusion. Figure PA-56 shows brine saturation in the waste panel (WAS_SATB for area Waste Panel in Figure PA-8) for replicate R1 of each BRAGFLO scenario. In many vectors, the intruded panel becomes saturated after an E1 intrusion (Scenarios S2, S3, and S6). Depending on the borehole permeability and pressures in the repository and in the brine reservoir, quantities of brine can flow from the reservoir into the intruded panel, possibly filling the panel. In contrast, after an E2 intrusion (Scenarios S4 and S5) saturation increases for only a few vectors. An E2 intrusion tends to reduce the pressure in the intruded panel by releasing fluids (mainly gas) up the borehole (Figure PA-49). The reduced pressure in the waste permits an increase in brine inflow from the DRZ and the MBs. In addition, in some vectors brine can flow down the borehole from the Culebra into the intruded panel, depending on the permeability of the borehole.***

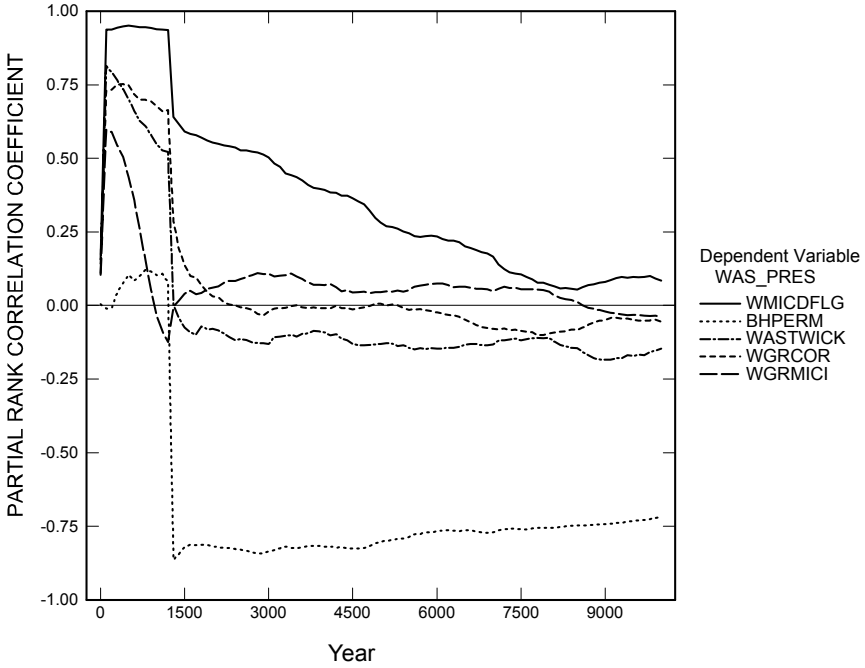


***Figure PA-54. Primary Correlations For Pressure In The Waste Panel With Uncertain Parameters, Replicate R1, Scenario S5.***

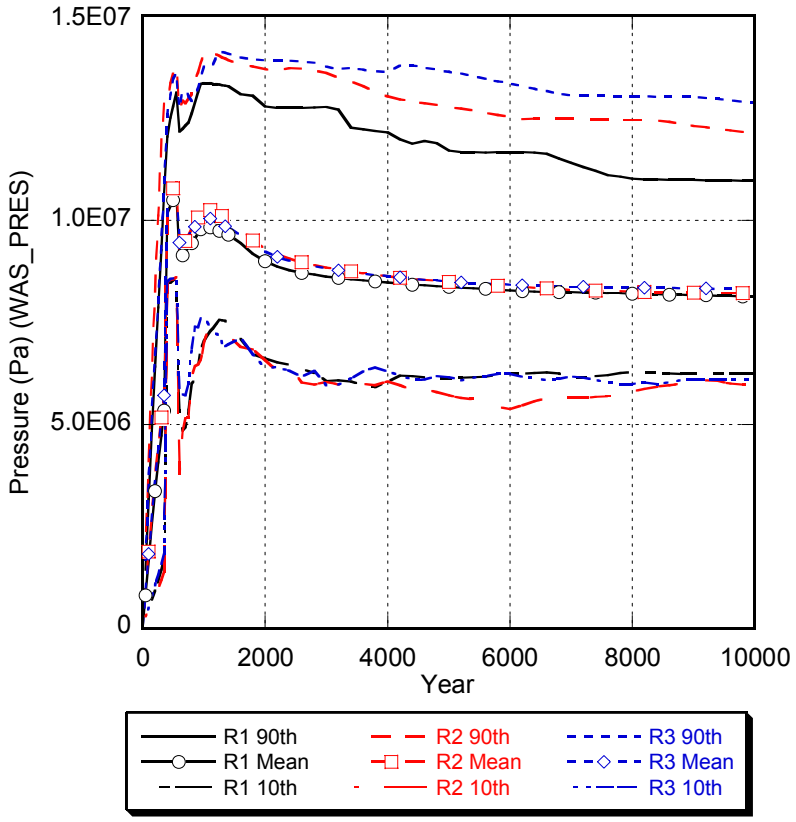


***Figure PA-55. Statistics For Pressure in the Waste Panel For All Replicates, Scenario S2.***

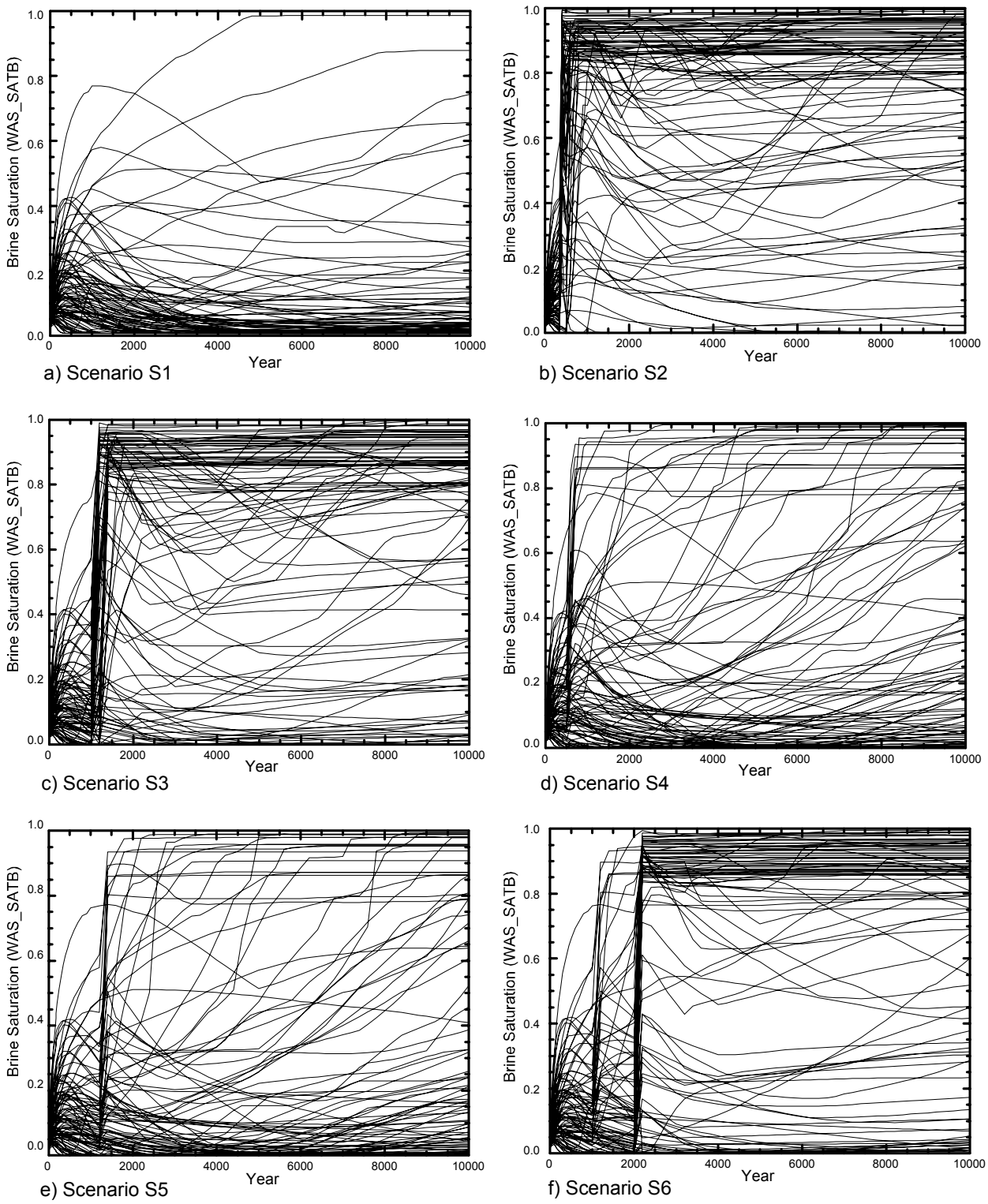


***Figure PA-56. Brine Saturation in the Waste Panel for All Scenarios, Replicate R1.***

***Figure PA-57 compares the mean values for brine saturation in the waste panel (WAS_SATB) for each scenario. Brine saturation is highest after E1 intrusions (Scenarios S2, S3, and S6), but also increases somewhat after an E2 intrusion (Scenarios S4 and S5). However, saturation in other excavated areas is not generally increased. Figure PA-58 shows brine saturation in the rest of repository (SRR_SATB for area South RoR and NRR_SATB for area North RoR in Figure PA-8) and in the nonwaste areas (NWA_SATB averaged over areas Ops and Exp in Figure PA-8) for the Scenarios S2 and S5. Comparison of Figure PA-57 with Figure PA-39, which shows brine saturation in undisturbed conditions, reveals that brine saturation in unintruded regions is generally unaffected by the intrusion. The panel closures separating the intruded panel from these regions effectively prevent brine flow between excavated areas. In addition, the intruded panel is modeled as one of the panels at the southern end of the repository, and hence is down the stratigraphic dip from the other excavated regions.***

***Figure PA-58 also shows that brine saturation in the nonwaste areas (areas Ops and Exp in Figure PA-8) is somewhat higher than in the rest of repository areas (areas South RoR and North RoR in Figure PA-8). Brine saturation in the nonwaste areas is higher because of the lack of brine consuming corrosion processes in these areas and their position adjacent to the northern marker beds, which supply brine to the excavated area. The rest of repository areas have the lowest saturations because they are not connected to the brine reservoir, corrosion consumes brine in these regions, and their internal position in the two-dimensional grid (Figure PA-8) prevents direct flow of brine from the MBs.***

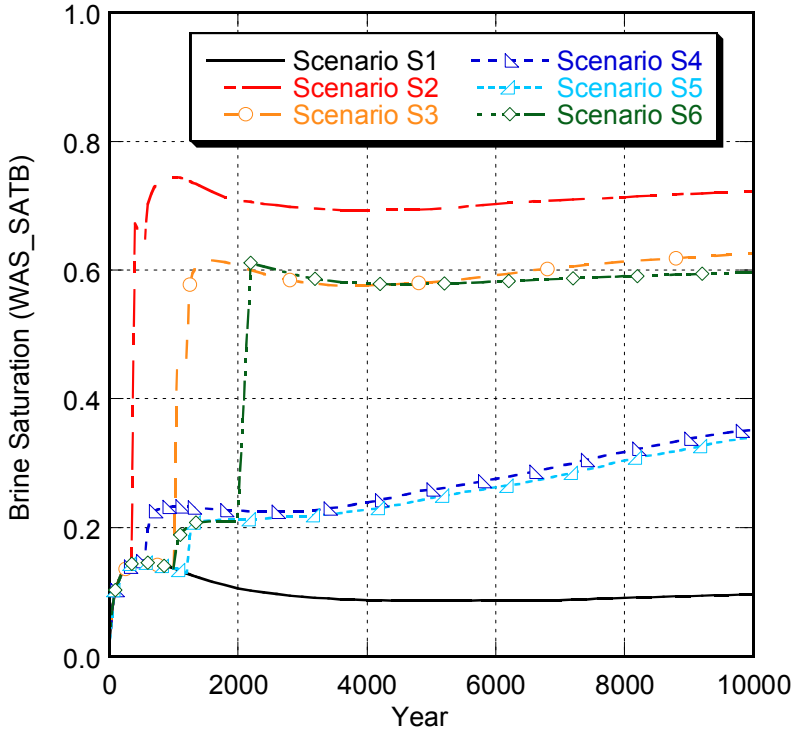


***Figure PA-57. Mean Values for Brine Saturation in the Waste Panel for All Scenarios, Replicate R1.***

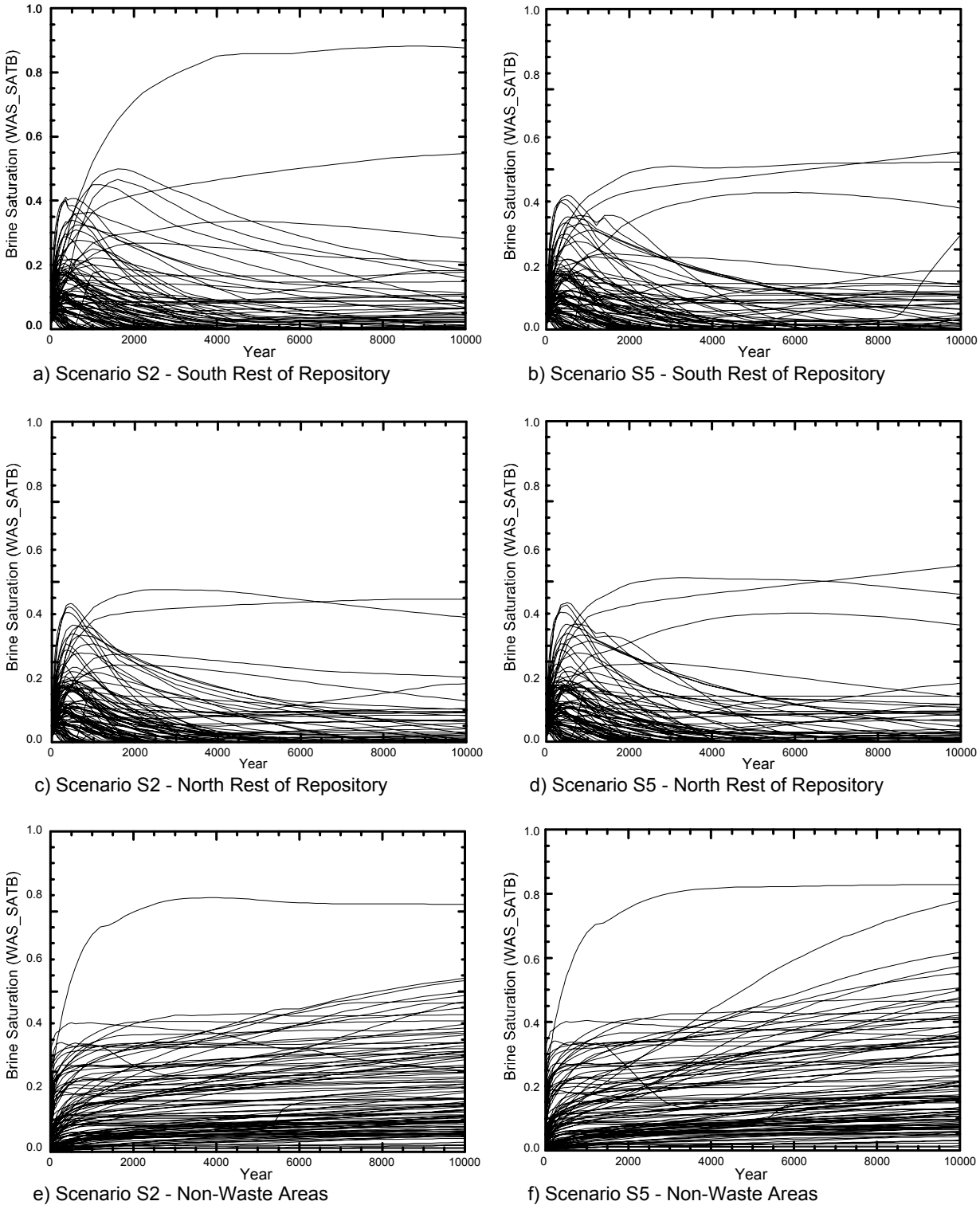


***Figure PA-58. Brine Saturation in Excavated Areas, Replicate R1, Scenarios S2 and S5.***

***Figure PA-59 compares mean and 90th percentile brine saturations among the excavated areas for an E1 intrusion at 350 years (Scenario S2). Brine saturations in the waste panel are the highest due to the connection with the brine reservoir. Comparison of Figure PA-59 to Figure PA-40, which shows mean pressure for undisturbed conditions, indicates that brine saturation outside of the waste panel is very similar to the undisturbed Scenario S1.***

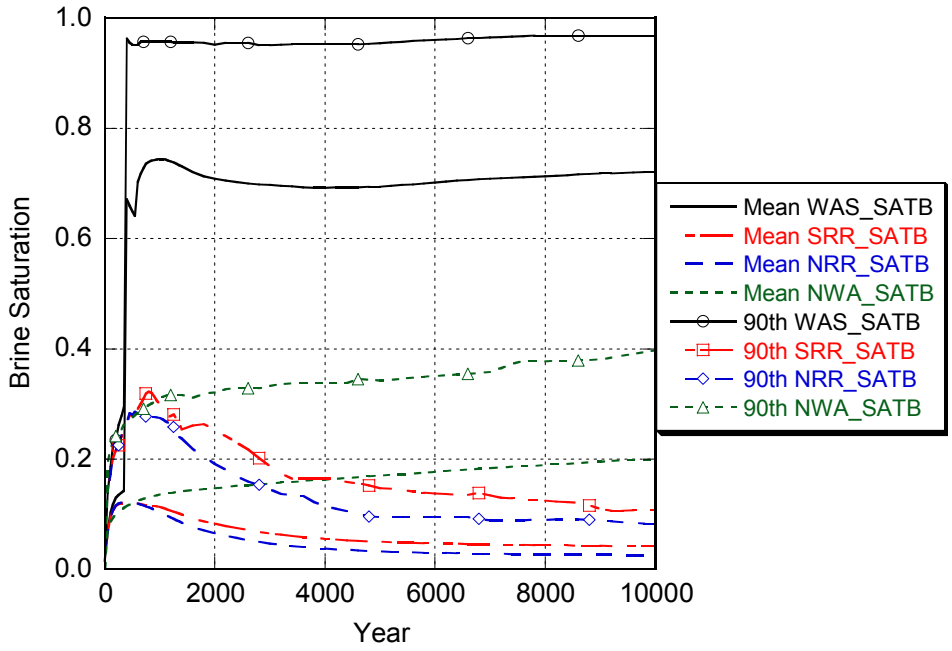


***Figure PA-59. Statistics For Brine Saturation in Excavated Areas, Replicate R1, Scenario S2.***

***Figure PA-60 shows the results of the regression analysis between brine saturation in the waste panel (WAS_SATB) for the S2 scenario and the uncertain parameters in the analysis (Section PA-5.2). For most of the time after the intrusion, uncertainty in borehole permeability (BHPERM) is primarily responsible for the uncertainty in brine saturation, with increases in borehole permeability leading to increases in brine saturation. The indicator for microbial degradation (WMICDFLG), which has a negative correlation with the brine saturation in the waste panel, also has a significant influence throughout the 10,000-year modeling period. Because the S2 scenario models an intrusion at 350 years, much of the CPR material is still present in the waste. Additional brine entering the waste panel would saturate more of the waste and accelerate the degradation of the CPR material, increasing gas pressure, and in turn retarding brine inflow. Thus, the negative correlation between the indicator for microbial degradation and brine saturation is quite strong immediately after the intrusion, but decreases in importance at later times. Uncertainty in the other parameters in Figure PA-60 (HALPOR, DRZPRM, and WGRCOR, defined in Table PA-17), have relatively little influence on brine saturation. Regression analysis of waste saturation for the S3 scenario yields a similar result (Stein and Zelinski 2003b).***

***Figure PA-61 shows the results of the regression analysis between brine saturation in the waste panel (WAS_SATB) for the S5 scenario and the uncertain parameters in the analysis (Section PA-5.2). As with the S2 scenario, borehole permeability is the primary factor***

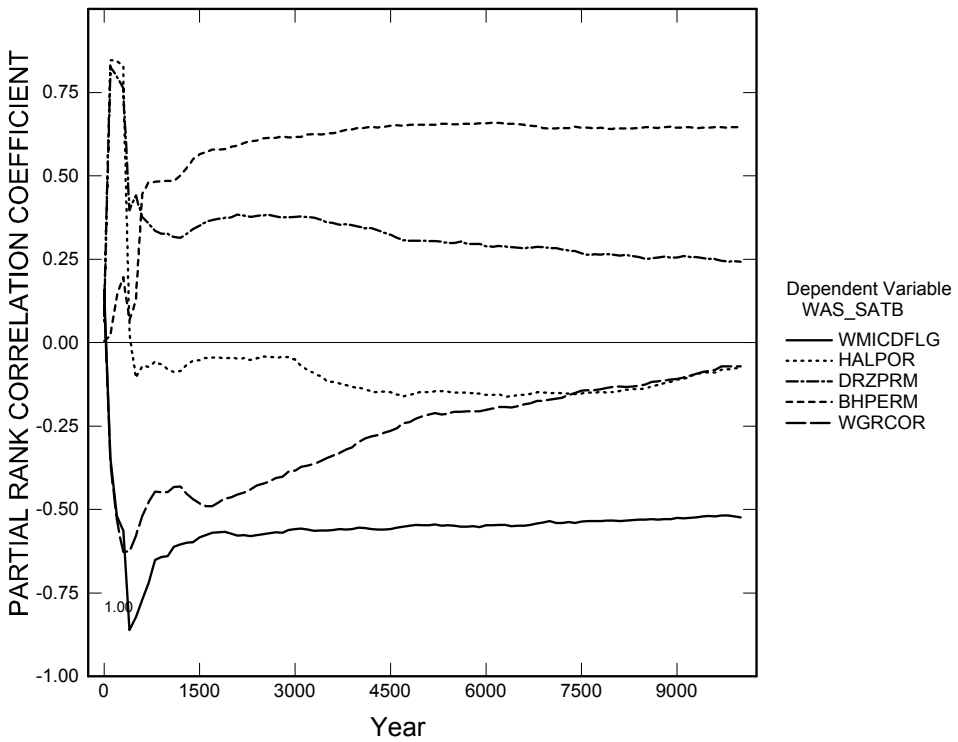


***Figure PA-60. Primary Correlations for Brine Saturation in the Waste Panel with Uncertain Parameters, Replicate R1, Scenario S2.***

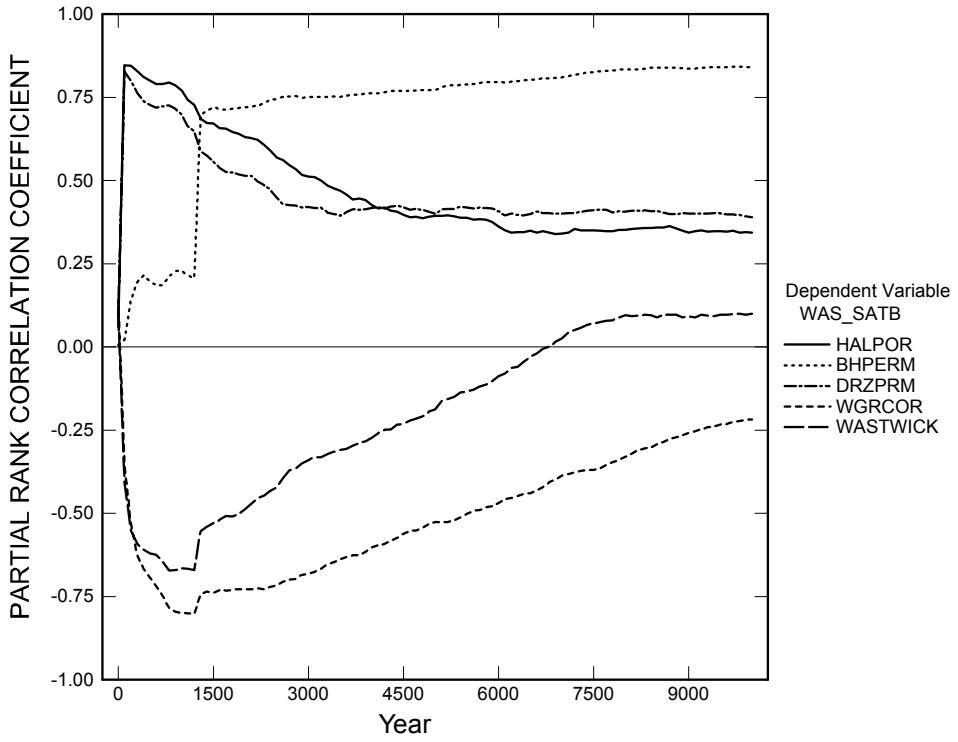


***Figure PA-61. Primary Correlations of Brine Saturation in the Waste Panel with Uncertain Parameters, Replicate R1, Scenario S5.***

***influencing brine saturation in the waste panel (WAS_SATB) after the borehole plugs fail. Regression analysis of waste saturation for the S4 scenario yields a similar result (Stein and Zelinski 2003b).***

***Figure PA-62 compares statistics for brine saturation for the three replicates of the S2 scenario, and shows that the replicates produced similar results.***

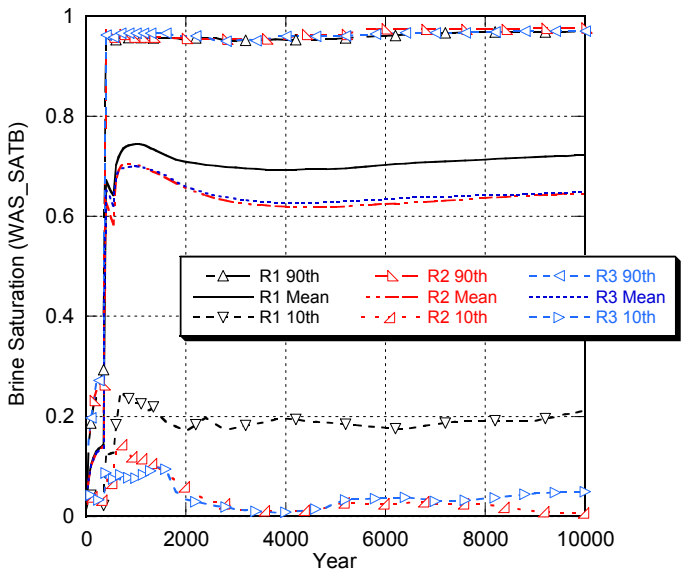


***Figure PA-62. Statistics for Brine Saturation in the Waste Panel For All Replicates, Scenario S2.***

### *PA-8.3.3 Brine Flow Out of the Repository*

***This section describes the flow of brine up a borehole to the Culebra. Brine flow to the Culebra is an important input to the calculations of long-term releases in the Culebra, described in Section PA-8.4.3. Direct brine flow up the borehole to the surface at the time of drilling is modeled separately in the DBR calculations, presented in Section PA-8.5.3.***

***Figure PA-63 shows cumulative brine flow out of the repository (BRNREPOC) and brine flow up a borehole to the Culebra (BRNBHRCC) for the five BRAGFLO scenarios that model drilling intrusions. The largest volumes of brine flow from the repository after E1 intrusions (Scenarios S2, S3, and S6), which is consistent with the higher brine saturation in the intruded panel (Figures PA-56b, PA-56c, and PA-56f, respectively). The similarity between the plots of BRNREPOC and BRNBHRCC indicate that nearly all the brine leaving the repository after an intrusion flows up the borehole to the Culebra. The few vectors that show brine flow out of the repository before the drilling intrusion generally have either very high pressures or very high DRZ permeability, allowing brine to flow from the repository into the MBs before the intrusion occurs. At 1,200 years after an E1 intrusion, the permeability of the borehole between the repository and the Castile is reduced by an order of magnitude because of creep closure (see Table PA-5), reducing brine flowing into the repository and causing a corresponding decrease in brine out of the repository.***

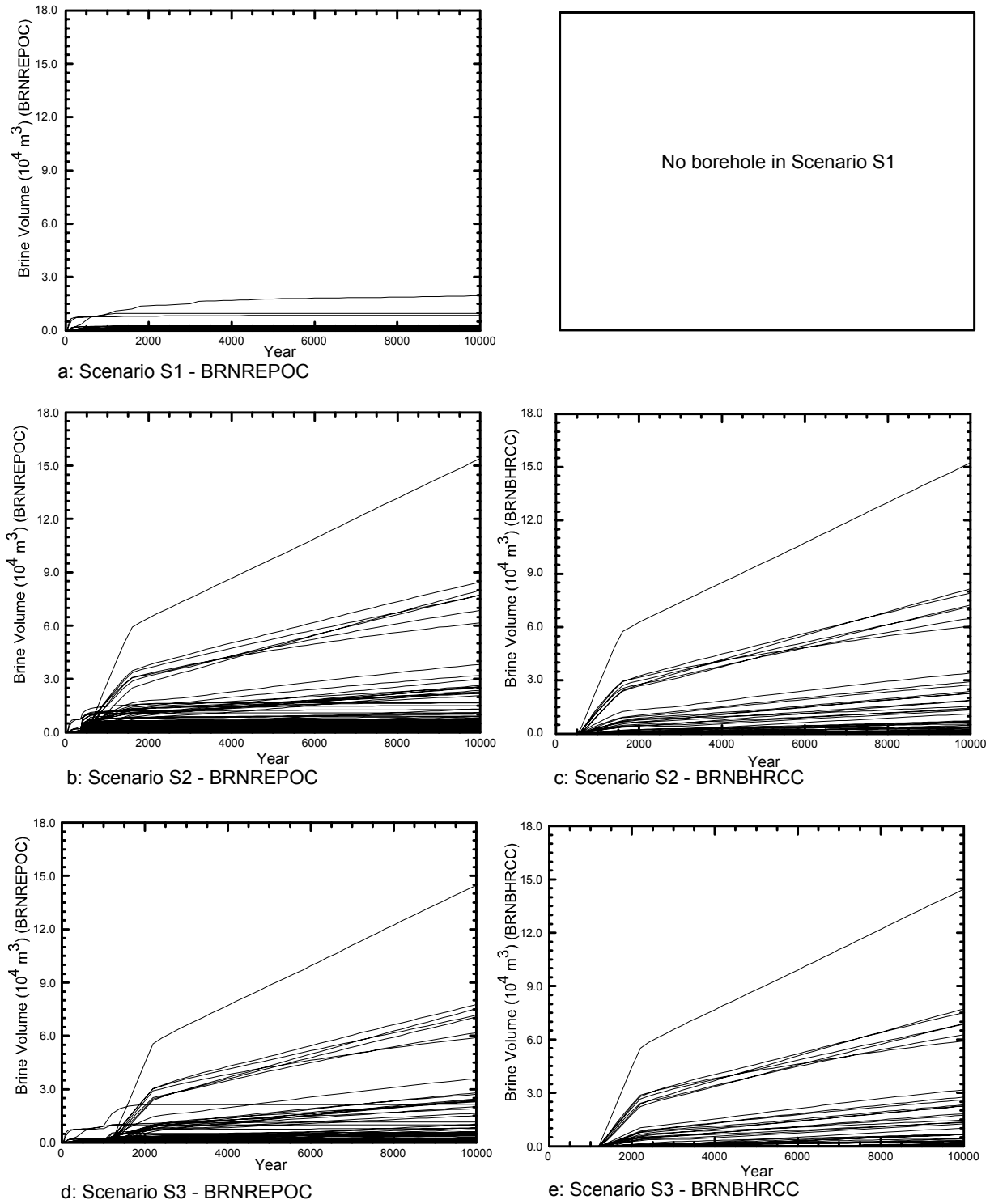


***Figure PA-63. Total Cumulative Brine Outflow and Brine Flow Up the Borehole in All Scenarios, Replicate R1.***

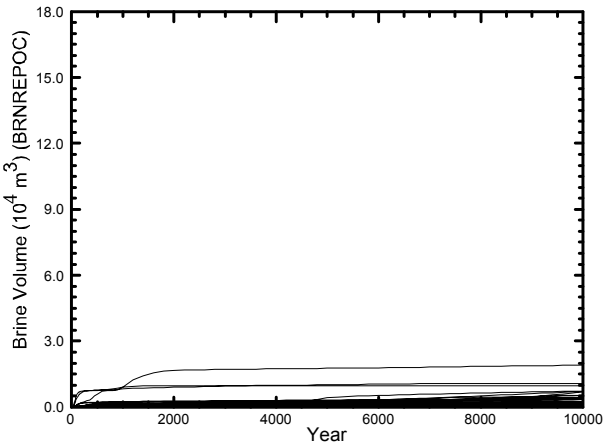


f) Scenario S4 - BRNREPOC

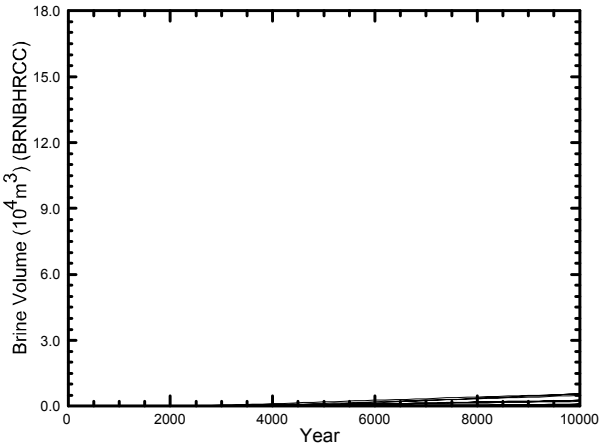


g) Scenario S4 - BRNBHRCC

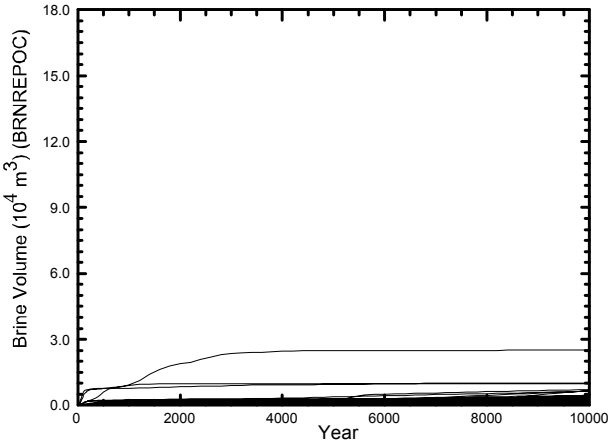


h) Scenario S5 - BRNREPOC

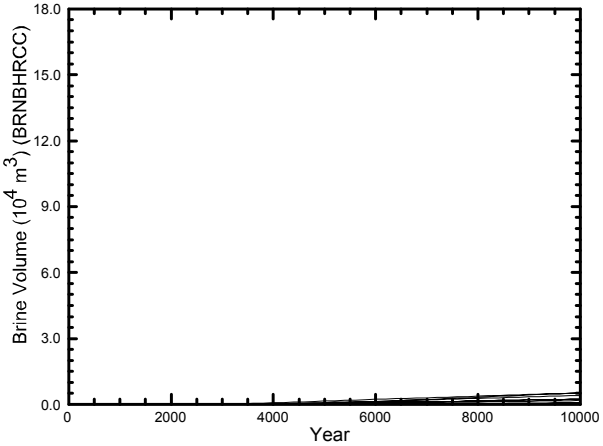


i) Scenario S5 - BRNBHRCC

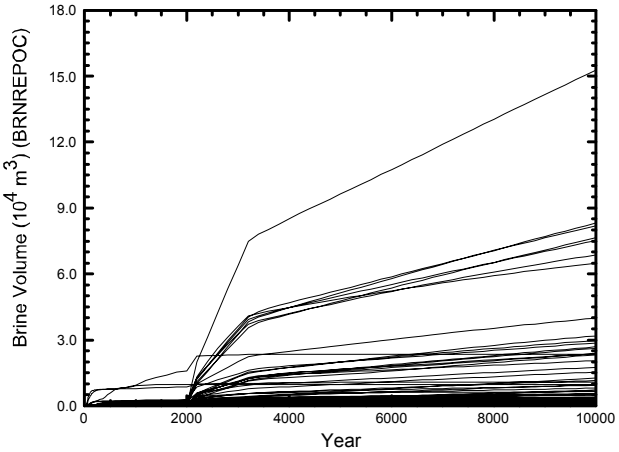


j) Scenario S6 - BRNREPOC

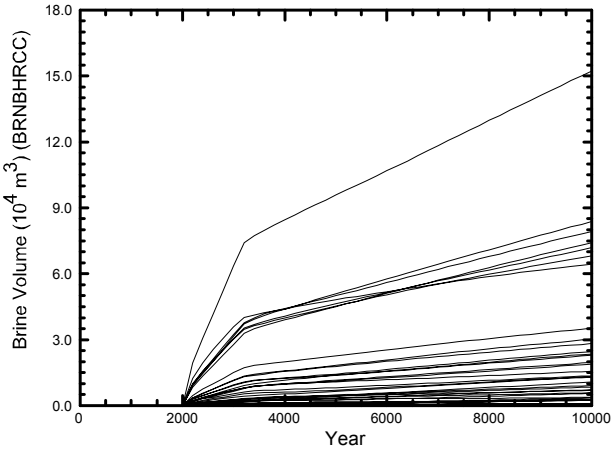


k) Scenario S6 - BRNBHRCC

***Figure PA-63(cont). Total Cumulative Brine Outflow and Brine Flow Up the Borehole in All Scenarios, Replicate R1***

***Figure PA-64 shows the results of regression analysis between the brine flow up the borehole to the Culebra (BRNBHRCC) and the uncertain parameters in the analysis (Section PA-5.2). Before the intrusion, non-zero values of BRNBHRCC result from numerical error in the calculation; these values do not exceed $10^{-18}$ $m^3$ and thus the correlation to uncertainty in shaft permeability (SHUPRM) is not meaningful. Immediately after the intrusion, uncertainty in the permeability of the undegraded borehole plugs (PLGPRM) contributes most of the uncertainty in brine flow volumes. After the borehole plugs degrade (200 years after the intrusion), uncertainty in the permeability of the borehole (BHPERM) almost exclusively determines the uncertainty in brine volumes reaching the Culebra. The indicator for microbial degradation (WMICDFLG) is weakly correlated with the small amount of uncertainty that is not explained by the uncertainty in borehole permeability.***

***Figure PA-65 compares statistics for brine flow out of the repository for the three replicates of Scenario S2. The figure shows that brine flow results are very similar among replicates.***

### *PA-8.4 Radionuclide Transport*

***In the disturbed scenarios, radionuclide transport in the Salado is calculated by the code NUTS (see Section PA-4.3). Transport from the Salado to the Culebra is calculated by NUTS and PANEL (see Section PA-4.3 and Section PA-4.4). Transport within the Culebra is calculated by SECOTP2D (see Section PA-4.9). For all transport calculations, mobilized concentrations of radionuclides in Salado and Castile brines are computed by the code PANEL (see Section PA-4.4).***

***This section summarizes the transport results for the disturbed scenarios. Detailed analysis of the NUTS results is presented in Lowry (2003). Garner (2003) provides analysis of the PANEL results; Kanney (2003) presents analysis of the SECOPT2D results.***

#### *PA-8.4.1 Radionuclide Source Term*

***The code PANEL calculates the source term for transport, which is the time-varying concentration of radioactivity mobilized in brine, either as dissolved isotopes or as isotopes sorbed to mobile colloids. Two different brines are considered: the interstitial brine present in the Salado Formation, which is magnesium rich; and the brine in the Castile Formation, which is sodium rich. Radionuclide solubility in the two brines can be considerably different. Before an E1 intrusion, performance assessment assumes that the brine in the repository is Salado brine. After an E1 intrusion, brine in the repository is assumed to be from the Castile.***

***Figure PA-66 and Figure PA-67 show the source term in Salado and Castile brines, respectively, as a function of time for all vectors in replicate R1. Concentrations are expressed as EPA units/$m^3$ to combine the radioactivity in different isotopes. Short-lived radionuclides, such as $^{238}Pu$, decay rapidly in the first few years. After this initial decay, the source term is dominated by Am (Garner 2003); the concentration of Am is limited by its solubility until all the inventory of Am is in solution. After all Am is in solution, the total radionuclide concentration generally decreases as the Am decays, until the source term becomes dominated by Pu (Garner 2003). The horizontal lines in the figures indicate periods of time when the***

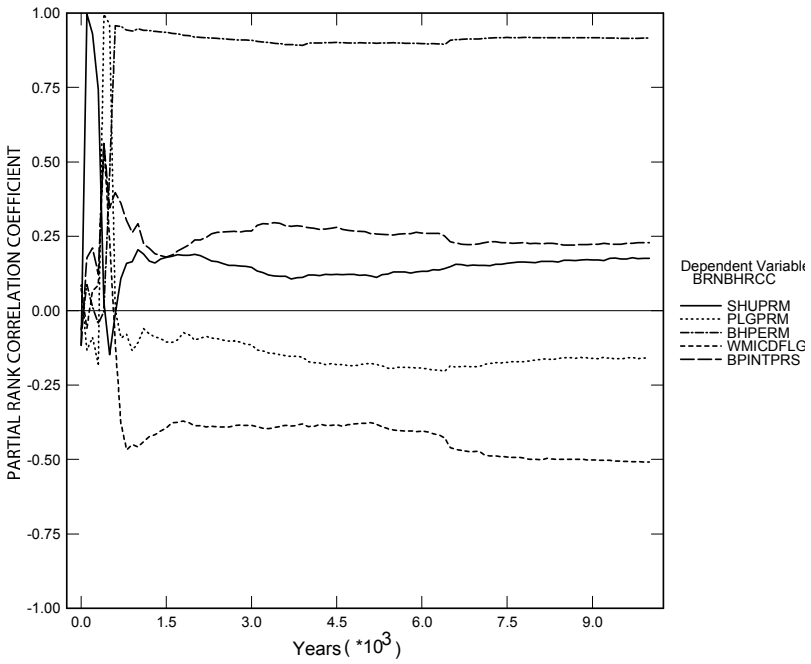


***Figure PA-64. Primary Correlations for Cumulative Brine Flow Up the Borehole with Uncertain Parameters, Replicate R1, Scenario S2.***

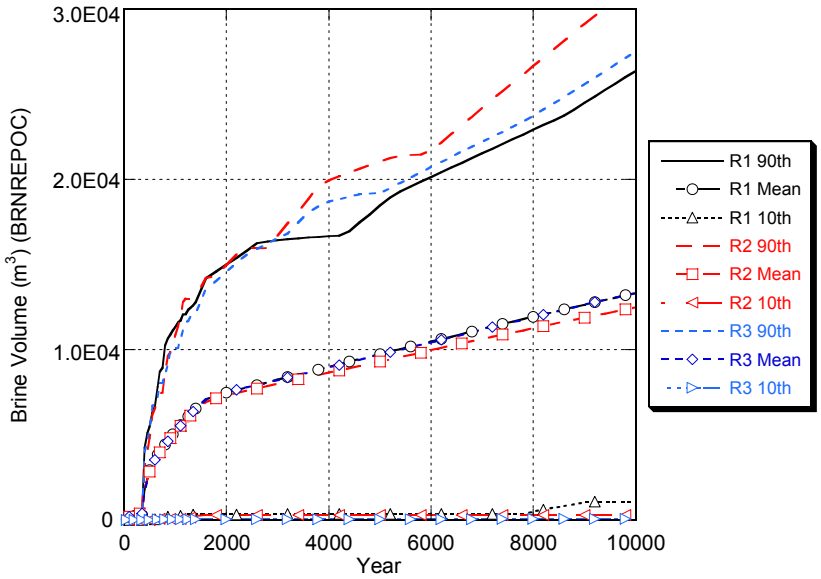


***Figure PA-65. Statistics for Cumulative Brine Outflow in All Replicates, Scenario S2.***

***total radionuclide concentration is limited by the solubility of Am (before about 3,000 years) or Pu (after about 6,000 years). Thus, the uncertainty in total radionuclide concentration is determined by the uncertainty factors used in the calculation of solubilities for Am and Pu (see Table PA-9).***

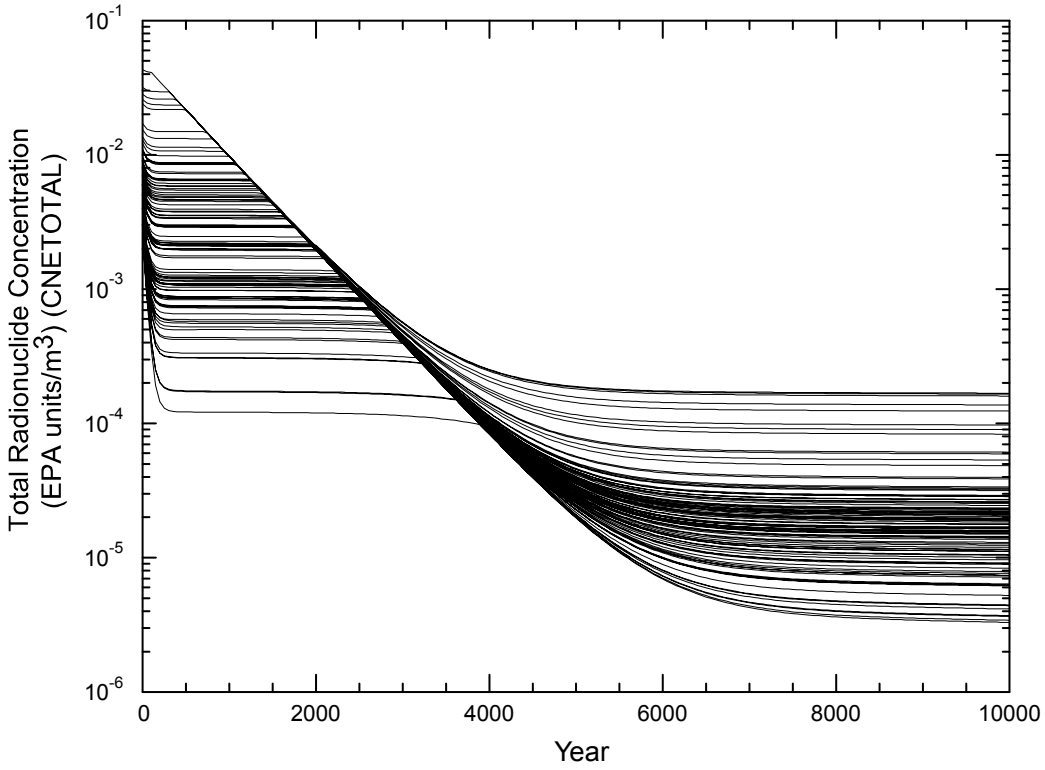


***Figure PA-66. Total Mobilized Concentrations in Salado Brine.***

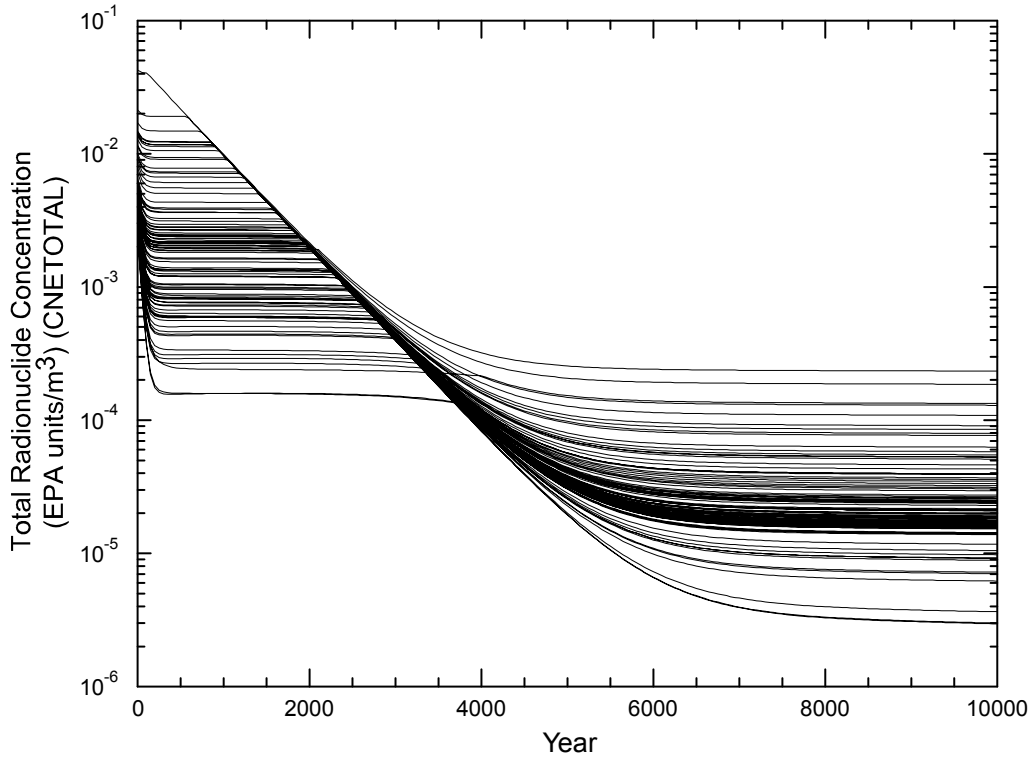


***Figure PA-67. Total Mobilized Concentrations in Castile Brine.***

### *PA-8.4.2 Transport through Marker Beds and Shaft*

***In the disturbed scenarios, none of the 300 realizations resulted in transport of radionuclides through the MBs and across the LWB (Lowry 2003). In addition, no realization showed transport of radionuclides through the shaft to the Culebra.***

### *PA-8.4.3 Transport to the Culebra*

***In four of the disturbed scenarios (S2, S3, S4, and S5), transport to the Culebra is modeled with the code NUTS. In the multiple intrusion scenario (S6), the code PANEL is used to calculate transport to the Culebra. Figures PA-68 through PA-71 show cumulative radioactivity transported up the borehole to the Culebra. Transport to the Culebra is larger and occurs for more vectors in the S2 and S3 scenarios (E1 intrusions) than in the S4 or S5 scenarios (E2 intrusions). For most vectors that show significant transport, most of the transport occurs over a relatively short period of time, immediately after the borehole plugs fail.***

***Figure PA-72 shows total EPA units transported to the Culebra via the borehole in the S6 scenario. Almost no radionuclides are released after the E2 intrusion at 800 years; most transport occurs immediately following the E1 intrusion at 2,000 years.***

***Figure PA-73 and Figure PA-74 compare mean values among all three replicates for cumulative normalized releases up the borehole to the Culebra for scenarios S3 and S6, respectively. These figures show that the results from each replicate are very similar.***

***Sensitivity analysis of total radionuclides transported to the Culebra identified a strong linear relationship between the uncertainty in the total release to the Culebra and the uncertainty in the brine flow up the borehole (calculated by BRAGFLO; see Section PA-8.3.3). Figure PA-75 shows the relationship between total releases to the Culebra (EPATBHRC, calculated by NUTS; see Section PA-4.3) and brine flow up the borehole (BRNBHRCC, calculated by BRAGFLO; see Section PA-8.3.3) at 10,000 years after an E1 intrusion at 1,000 years (Scenario S3). Figure PA-76 shows the relationship between total releases to the Culebra (LDETOTAL, calculated by PANEL; see Section PA-4.4) and brine flow up the borehole (BRNBHRCC, calculated by BRAGFLO; see Section PA-8.3.3) at 10,000 years after the combination of an E2 intrusion at 800 years followed by an E1 intrusion in the same panel at 2,000 years (Scenario S6).***

***Sensitivity analysis (Section PA-8.3.3) identified borehole permeability (BHPERM) as the most important parameter contributing to the uncertainty in flow up the borehole (BRNBHRCC). Separate stepwise regression analyses (Lowry 2003; Garner 2003) confirmed the correlation between uncertainty in borehole permeability and releases to the Culebra. These analyses also identified the initial pressure in the brine pocket (BPINTPRS), indicator for microbial action (WMICDFLG), and steel corrosion rate (WGRCOR) as contributing to uncertainty in releases to the Culebra although the importance of these parameters is much less than that of borehole permeability.***

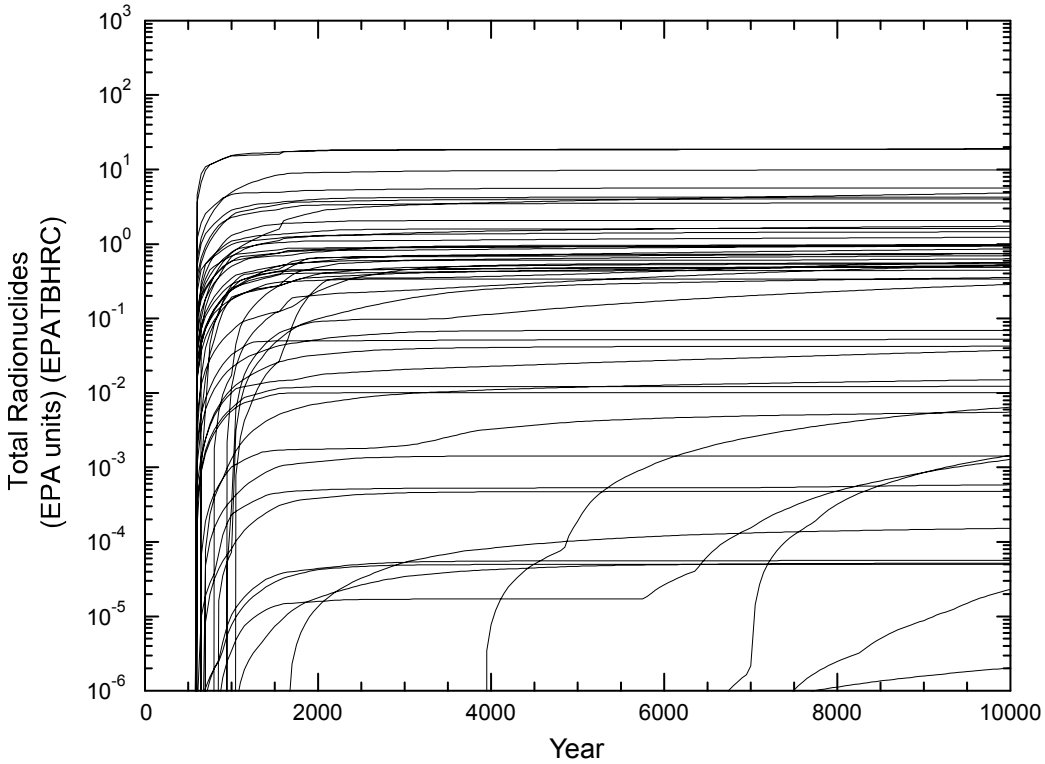


***Figure PA-68. Cumulative Normalized Release Up the Borehole, Replicate R1, Scenario S2.***

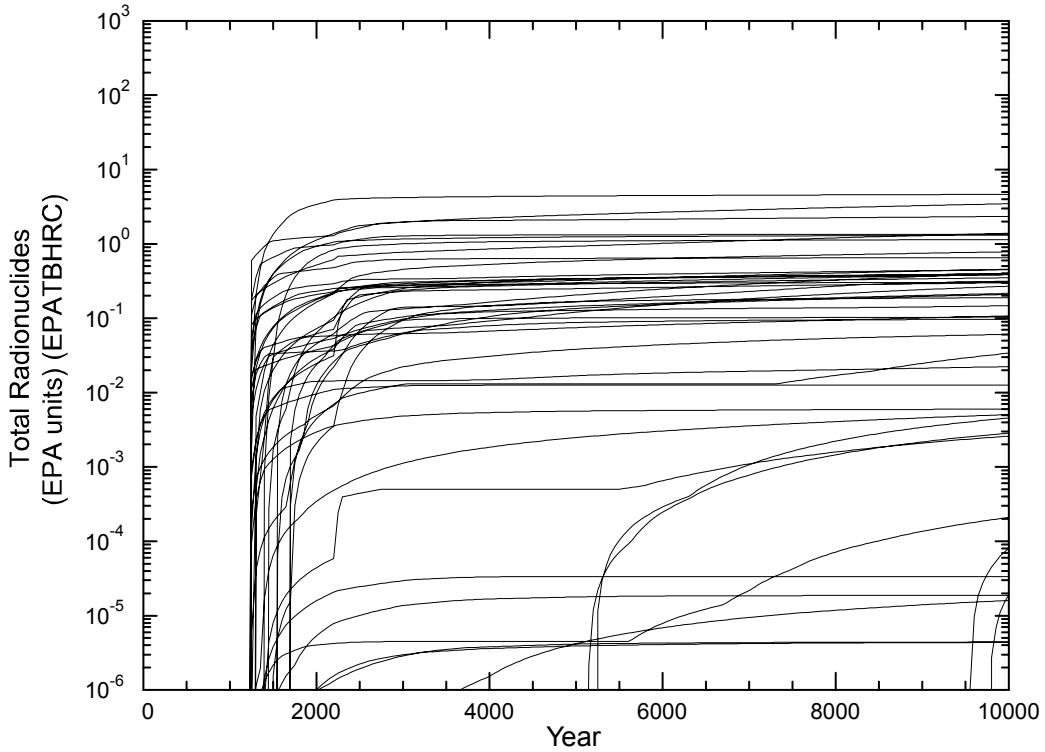


***Figure PA-69. Cumulative Normalized Release Up the Borehole, Replicate R1, Scenario S3.***

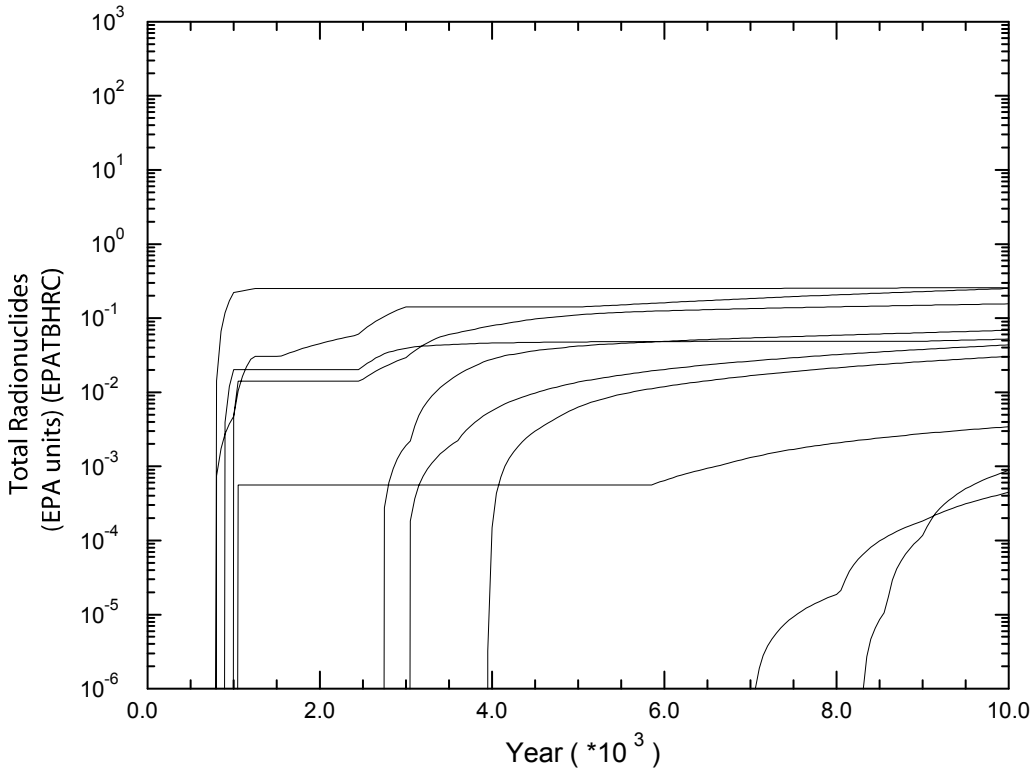


***Figure PA-70. Cumulative Normalized Release Up the Borehole, Replicate R1, Scenario S4.***

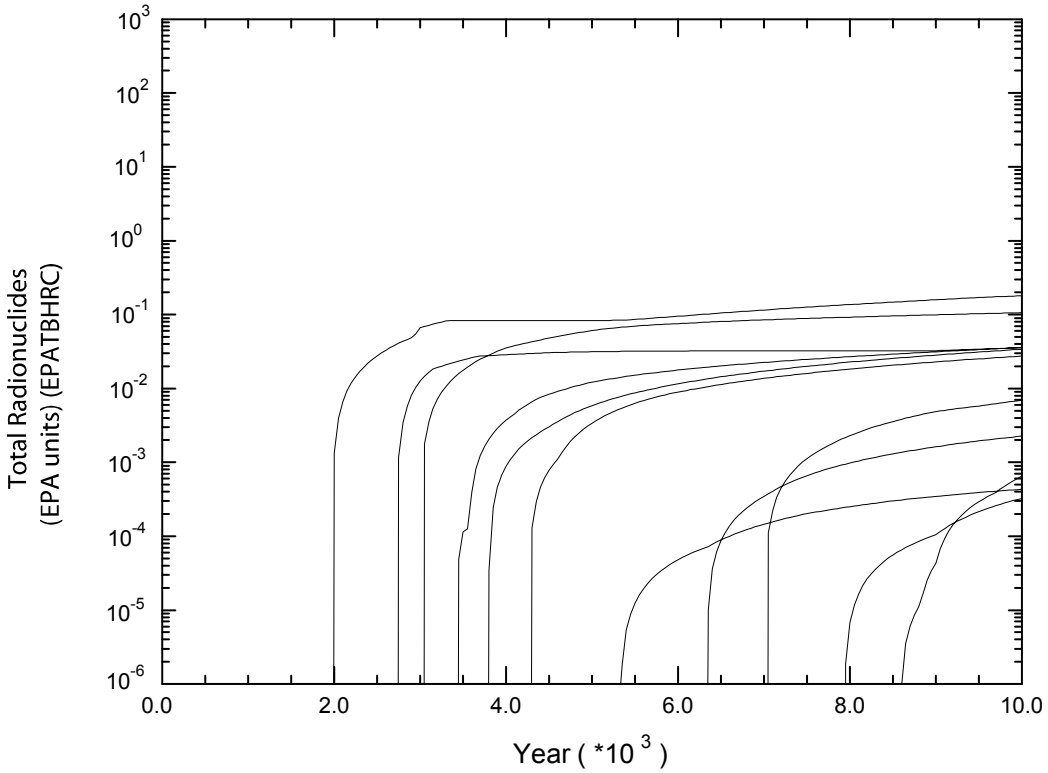


***Figure PA-71. Cumulative Normalized Release Up the Borehole, Replicate R1, Scenario S5.***

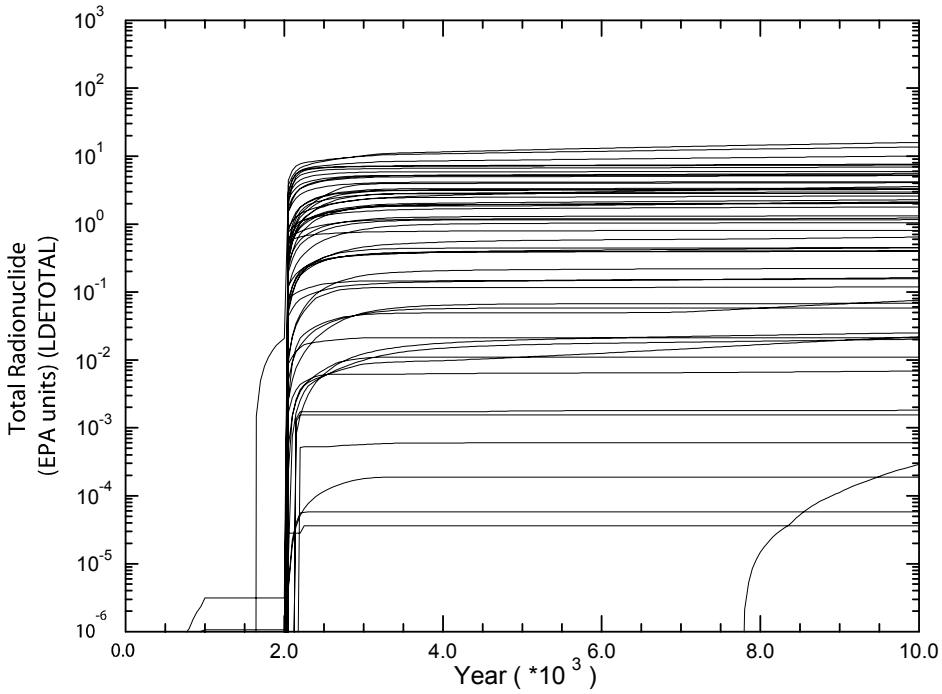


*Figure PA-72. Cumulative Normalized Release Up the Borehole, Replicate R1, Scenario S6.*

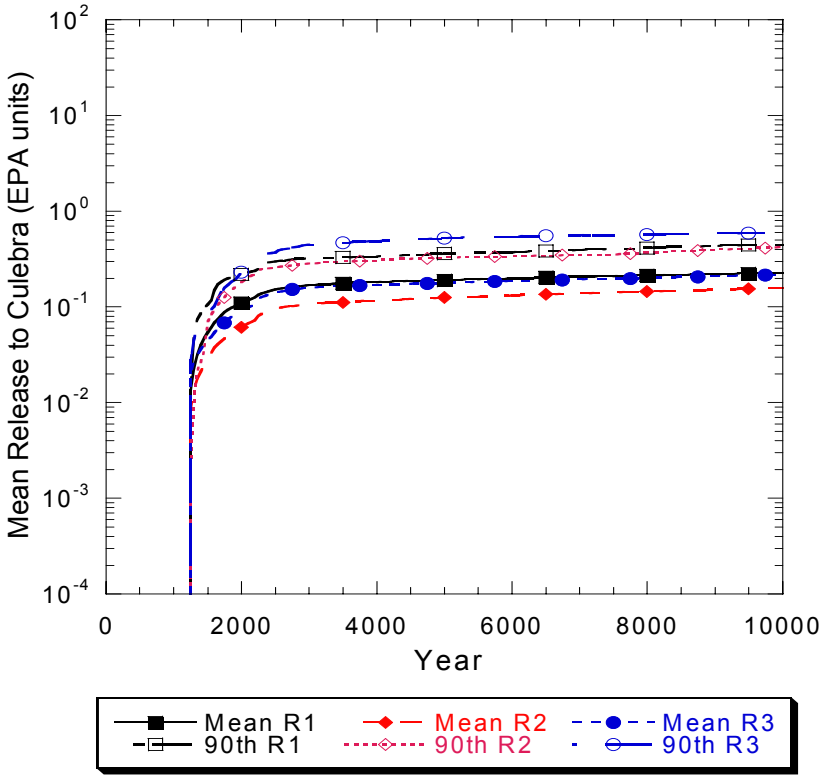


*Figure PA-73. Mean Values for Cumulative Normalized Release Up the Borehole for All Replicates, Scenario S3.*

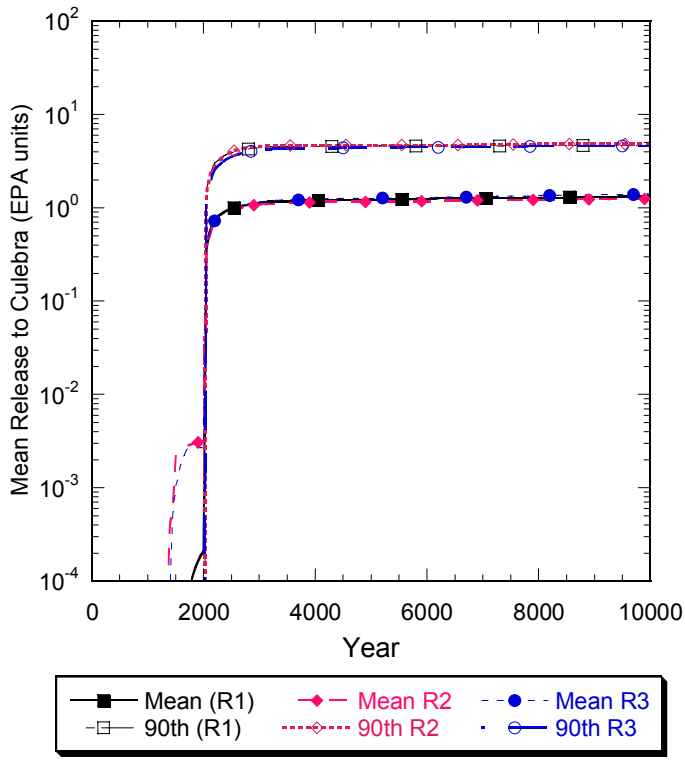


***Figure PA-74. Mean Values for Cumulative Normalized Release Up Borehole for All Replicates, Scenario S6.***

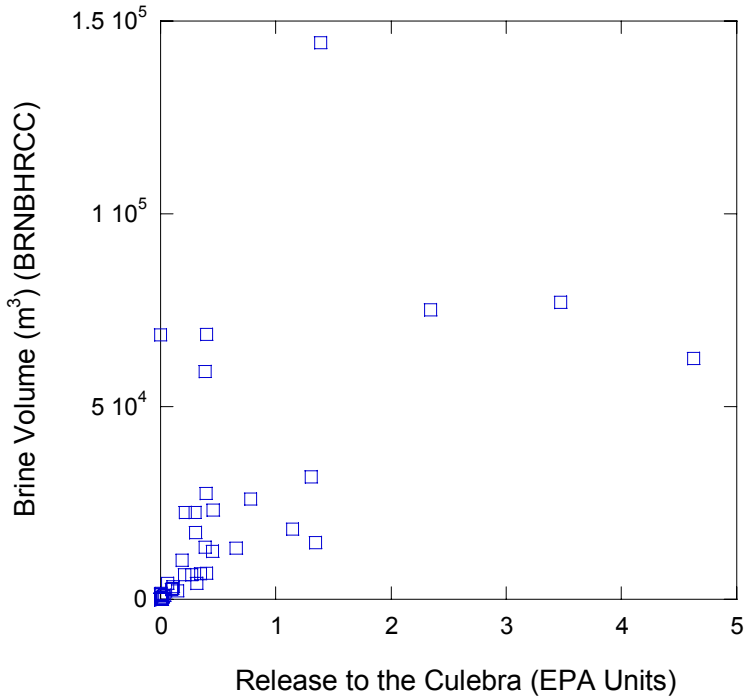


***Figure PA-75. Comparison of Total Release to Culebra with Flow Up Borehole, Replicate 1 Scenario S3.***

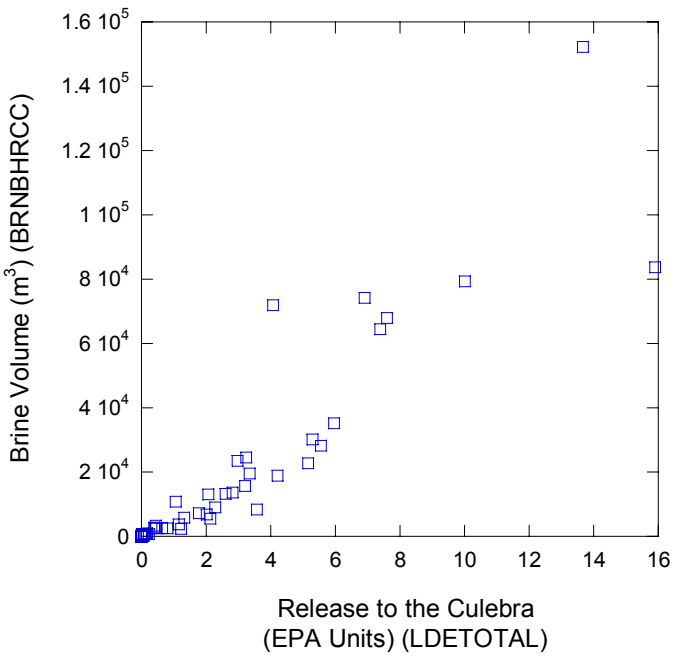


***Figure PA-76. Comparison of Total Release to Culebra with Flow Up Borehole, Replicate 1 Scenario S3.***

### *PA-8.4.4 Transport through the Culebra*

***Releases through the Culebra are calculated with the code SECOTP2D (see Section PA-4.9). As explained in Section PA-6.8.7, transport through the Culebra is calculated for a release of 1 kg of each of four radionuclides ($^{241}$Am, $^{234}$U, $^{230}$Th, and $^{239}$Pu). Am is present as Am(III) and Th as Th(IV). Uranium may be present as either U(IV) or U(VI); plutonium may be present as Pu(III) or Pu(IV). The oxidation state of uranium and plutonium is an uncertain parameter (see WOXSTAT in Table PA-17). The total release of radionuclides across the LWB at the Culebra is calculated by the code CCDFGF by convoluting the SECOTP2D results with the transport to the Culebra calculated by NUTS and PANEL. This section discusses the SECOTP2D results; releases through the Culebra are presented in Section PA-9.5.***

***Transport calculations were performed for both partial-mining and full-mining scenarios. The partial-mining scenario assumes the extraction of all potash reserves outside the LWB while full mining assumes that all potash reserves both inside and outside the LWB are exploited. Flow fields in the Culebra are computed separately for each mining scenario by the code MODFLOW (see Section PA-4.8).***

***All SECOTP2D results, regardless of magnitude, are included in the calculation of releases through the Culebra. In practice, most non-zero releases computed by SECOTP2D are vanishingly small and result from numerical error (Kanney 2003). Consequently, the analysis of SECOTP2D results focused on realizations in which at least one billionth ($10^{-9}$) of the 1 kg source was transported to the land withdrawal boundary.***